A review of experimental investigations on salt precipitation during CO2 geological storage

Xiaolong Sun[a,b*], Keyu Liu[a,b], Senyou An[c*], Helge Hellevang[d], Yingchang Cao[a,b], Juan Alcalde[e], Anna Travé[f], Guanghui Yuan[a,b], Chenguang Deng[a], Enrique Gomez-Rivas[f]

[a] School of Geosciences, China University of Petroleum (East China), Qingdao 266580, China

[b] State Key Laboratory of Deep Oil and Gas, China University of Petroleum (East China), Qingdao 266580, China

[c] Shenzhen Key Laboratory of Deep Engineering Sciences and Green Energy, Shenzhen University, Shenzhen 518060, China

[d] Department of Geosciences, University of Oslo, Oslo 0316, Norway

[e] Geosciences Barcelona (GEO3BCN), CSIC, Barcelona 08028, Spain

[f] Department of Mineralogy, Petrology and Applied Geology, University of Barcelona, Barcelona 08028, Spain

This is an authors' version of the article published in:
Sun et al. (2025). A review of experimental investigations on salt precipitation during CO_2 geological storage. *Geoenergy Science and Engineering*, 244, 213451.
DOI: https://doi.org/10.1016/j.geoen.2024.213451

Abstract: Salt precipitation due to formation drying is a critical secondary alteration process that significantly impairs reservoir injectivity in the context of CO_2 geological storage. In this work, salt precipitation during CO_2 injection is reviewed primarily through various experimental studies. First, the experimental systems for salt precipitation studies, namely core-flooding, microfluidic-chip, static batch, and surface drying experimental systems, have been described to present their respective experimental procedures and merits, as well as corresponding applications. Subsequently, following the general description of the formation mechanisms of salt precipitation, the macro and micro salt distribution patterns at the reservoir and pore scales have been summarized. Finally, and most importantly, this study provides a comprehensive analysis of the controlling factors for salt precipitation, categorized into four different groups, according to the brine, rock, gas, and injection scenario aspects. Among all these factors, brine salinity, CO_2 injection rate and initial reservoir properties are considered the most critical in determining the amount and distribution of precipitated salts and the degree of injectivity impairment. The effects of multi-scale reservoir heterogeneity and rock wettability on salt precipitation are attracting growing consideration, while the brine and gas composition studies are receiving less attention due to their relatively minor influences on reservoir alteration. Due to the limited specimen sizes, the ex-situ brine replenishment may be underestimated in core-flooding and microfluidic-chip experiments. This may result in a potentially significant underestimation of the volume of local salts and the potentially inaccurate prediction of the drying process during CO_2 injection in many such experiments.

Keywords: CO_2 storage; salt precipitation; evaporation; reservoir injectivity; experimental study.

1 Introduction

Carbon capture and storage (CCS) has been widely considered a promising technology for global net zero emissions of carbon (Alcalde et al., 2018; Budinis et al., 2018; Bui et al., 2018; IPCC, 2018; Sun et al., 2020). Around two hundred parties have submitted their Nationally Determined Contributions (NDC) to the Paris Agreement to describe their strategies for climate change mitigation (UNFCCC, 2022). More than forty countries include CCS technology in their national carbon neutrality plans (Sun et al., 2021). However, CCS development has stalled in many regions due to several main barriers, such as high development cost perception and potential safety issues (Leung et al., 2014; Budinis et al., 2018; Bui et al., 2018).

The safety and efficiency of the CO_2 geological storage (CGS) operations are essential to make CCS commercially and environmentally sustainable, and socially acceptable. Among the CGS chain of activity, finding the most suitable and potential storage site is a crucial step. A promising storage candidate must include a suitable emission source-geologic sink matching, sufficient storage capacity, reliable containment efficiency, and sustained reservoir injectivity (Miri and Hellevang, 2016; Aminu et al., 2017; Alcalde et al., 2021). Among these criteria, sustained reservoir injectivity ensures high injection rates of CO_2 at acceptable injection pressures. Achieving suitable injectivity rates reduces the development costs of CGS by minimizing the number of injection wells and energy requirements, while also lowering leakage risks by preserving well and formation integrity through reduced injection pressure. A potential storage site generally features high injectivity when it has thick reservoirs with high initial permeability. However, injectivity can be reduced by a series of secondary alterations in the reservoir due to injection operations, including clay swelling, mineral precipitation, fines migration, and/or borehole deformation (Torsæter and Cerasi, 2018; Hajiabadi et al., 2021; Ngata et al., 2023).

During CO_2 storage, mineral precipitation can result from various CO_2-brine or CO_2-brine-rock interactions. Salt precipitation is of particular concern because it occurs rapidly near injection wellbores driven by fast precipitation kinetics. With the continuous injection of CO_2, the remnant formation brines gradually reach oversaturation due to water evaporation into the CO_2 stream. Finally, salts precipitate and result in pore-throat blockage and injectivity impairment. This phenomenon has been disclosed from field deployment projects, such as the Ketzin project in Germany (Baumann et al., 2014), the Snøhvit project in Norway (Grude et al., 2014), and the Boundary Dam project in Canada (Talman et al., 2020). Furthermore, a number of experimental and numerical simulation studies have been carried out to reveal the mechanisms of salt precipitation, the effects on CO_2 injectivity, and the potential mitigation strategies. Miri and Hellevang (2016) presented a review that systematically summarizes the research outcomes published up to 2015. Since then, numerous subsequent studies have been published. Thus, in this contribution, we mainly focus on the more recent experimental studies of salt precipitation, and additionally refer to some numerical simulation results, with the overarching aim of providing an overview of the state-of-the-art on salt precipitation during CO_2 storage.

2 Experimental methodology

There are two widely used experimental approaches for mimicking salt precipitation during CGS, namely core-flooding experiments and microfluidic-chip experiments. The former enables 3D core-scale studies, while the latter focuses on 2D pore-scale studies. In addition, static batch experiments and surface drying experiments are also adopted to investigate salt precipitation processes in the context of CGS.

2.1 Core-flooding experiment system

The core-flooding system is the most frequently used method to investigate salt precipitation during CO_2 injection. To review date, more than thirty peer-reviewed publications have adopted this method to study salt precipitation during CGS (Muller et al., 2009; Wang et al., 2009, 2010, 2019, Ott et al., 2011, 2013, 2014, 2015, 2021, Peysson et al., 2011a, 2011b, 2014; Bacci et al., 2011; Vanorio et al., 2011; Bacci et al., 2013; Van Hemert et al., 2013; Roels et al., 2014, 2016; Jeddizahed and Rostami, 2016; Sokama-Neuyam et al., 2017a, 2019, 2023; Sokama-Neuyam and Ursin, 2018; Berntsen et al., 2019; Lopez et al., 2020; Md Yusof et al., 2020; Falcon-Suarez et al., 2020; Jayasekara et al., 2020; Akindipe et al., 2021; Lima et al., 2021; Akindipe et al., 2022; Abbasi et al., 2022; Mat Razali et al., 2022; Edem et al., 2022).

The experimental preparation work mainly includes core specimen preparation with different sizes, lithologies, and initial physical properties, as well as synthetic brine preparation with different salinities and salt compositions. Generally, the initial physical properties of the core specimen, such as porosity, permeability, pore structure or mechanical characteristics, are measured before and/or during the core-flooding experiment. Subsequently, the specimen is typically wrapped with aluminum foil, shrinking sleeve and rubber sleeve from the inside out to prevent CO_2 leakage. It is then mounted into the core holder of the displacement apparatus, vacuumed to exhaust air gas, and saturated with synthetic brine. To avoid any residual air in the specimen preventing the complete saturation of brine, a potential pretreatment includes fully displacing the air with CO_2 before applying the vacuum (Van Hemert et al., 2013; Roels et al., 2014, 2016, Akindipe et al., 2021, 2022). In this case, any residual gas will be replaced by CO_2 and the potential residual CO_2 can be removed through dissolution into the continuously injected brine. Afterward, supercritical CO_2 ($scCO_2$) is injected into the specimen at different rates to displace and evaporate brine under high temperature and pressure conditions, ultimately resulting in salt precipitation during the specimen dry-out. Some experiments have used CO_2 gas at ambient temperature or low-pressure conditions due to limitations of the experimental apparatus (Van Hemert et al., 2013; Roels et al., 2014, 2016; Falcon-Suarez et al., 2020), while others replaced CO_2 with N_2/He/air for security considerations or to avoid equipment corrosion by acidic fluids (Peysson et al., 2011b, 2014; Peysson, 2012; Lopez et al., 2020; Mascle et al., 2023).

The above experimental processes simulate general CO_2 injection into saline aquifers, while some other experiments employed special procedures to imitate more complex CO_2 injection scenarios. For instance, Bacci et al. (2011) conducted a multi-cycle experiment to imitate a long-term intermittent CO_2 injection through cyclic brine saturation-CO_2 displacement and evaporation. Ott et al. (2013, 2021) and Akindipe et al. (2022) used core specimens saturated with both oil and brine for CO_2 flooding to represent CO_2 injection into oil or depleted oil reservoirs. Additionally, although some studies used CH_4 to simulate salt precipitation in a gas storage scenario (e.g., Golghanddashti et al., 2013; Tang et al., 2023), these experimental results could also apply to cases of salt precipitation during CO_2 injection into gas or depleted gas reservoirs.

During the entire core-flooding experiment, the distribution of brine, CO_2 and salt can be determined using micro-CT scanning of the whole or part of the core specimen at different experiment stages, such as during the vacuum, brine saturation, displacement and drying stages. The use of X-ray monitoring alone is, however, not sufficient to de-correlating and quantifying local water saturation, salt concentration and qualities of salt precipitation, because X-ray contrast is sensitive to all material variations including water saturation and salt concentration. Therefore, Mascle et al. (2023) adopted a new in-situ monitoring instrument to simultaneously acquire X-ray and Neutron radiographies. This approach enables the quantitative separation of different phase saturations as well as brine salinity thanks to their different attenuation characteristics. Br, I or Cs salts were used in some experiments instead of Cl salts to improve the X-ray contrast between CO_2 and brine or salt, helping to better distinguish different phases (Van Hemert et al., 2013; Ott et al., 2014, 2015, Roels et al., 2014, 2016, Akindipe et al., 2021, 2022; Mascle et al., 2023). To limit brine/CO_2 backflow and maintain quasi-static conditions during high-resolution image acquisition, Akindipe et al. (2021, 2022) kept brine or CO_2 injection at a very low rate during each X-ray scanning period.

In addition to the monitoring of brine, CO_2 and salt distributions, injected rates and pressure profiles can be detected through equipped flowmeters or pressure transducers to obtain real-time changes of permeability. Dehydration rates, including displaced water and evaporated water, can be calculated not only through the detection of residual water in the core specimen but also through the measurement of water loss. Liquid water loss can be directly collected and weighted from effluents. The gaseous water loss can be collected through silica-gel packs, to then calculate the evaporation rate based on the weight variation of the silica-gel packs (Golghanddashti et al., 2013; Jeddizahed and Rostami, 2016; Abbasi et al., 2022). Apart from tests during the core-flooding process, valuable data can also be obtained through various post-flooding tests, including salt distribution, mineralogical characteristics, and core physical properties. These data can be obtained using X-ray diffraction (XRD), scanning electron microscopy with energy dispersive spectroscopy (SEM-EDS), mercury intrusion porosimetry (MIP), nuclear magnetic resonance (NMR), etc. Finally, based on the comprehensive analysis of the results from the experiments described above, the salt precipitation processes, salt distribution patterns, and the subsequent injectivity impairment can be determined. If the core specimens need to be used to conduct more experiments, they can be cleaned through core-flooding by deionized water or low salinity water and then ethanol flooding (Jeddizahed and Rostami, 2016).

2.2 Microfluidic-chip experiment system

The microfluidic-chip system is the other most commonly used method. More than ten peer-reviewed publications adopted this method to study salt precipitation during CGS to review date (Kim et al., 2013; Miri et al., 2015; Rufai and Crawshaw, 2017, 2018; Nooraiepour et al., 2018; He et al., 2019, 2022; Seo et al., 2019; He et al., 2024; Ho and Tsai, 2020; Hu et al., 2022; Wang et al., 2024).

Although the microfluidic-chip experiment system generally follows a similar experimental procedure to the core-flooding approach, it presents significant differences across the different experimental stages, particularly in terms of preparation work and process monitoring methods. On the one hand, compared to the core-flooding system, which uses readily available natural rock samples, the microfluidic-chip system requires the more labor-intensive initial step of chip fabrication. A 2D chip, generally shaped as a rectangle, consists of a substrate plate and a cover plate, and is usually made of silicon glass. The chips are usually made of Poly(methyl methacrylate) (PMMA) or Polydimethylsiloxane (PDMS) due to their chemical resistance and mechanical stability (e.g., Kim et al., 2013; Seo et al., 2019; Ho and Tsai, 2020). The

substrate is etched by a laser ablation system or by a chemical etching method, such as hydrofluoric acid, to obtain a pore-throat network or a pore-fracture network. Then, the substrate and cover plates are bonded together using a thermal or chemical bonding method. In addition to 2D chips, 1D channels have also been used to simulate salt precipitation in a single pore or a single pore-throat configuration, such as a single channel (Miri et al., 2015) or a straight channel with an isolated pore (Kim et al., 2013). Moreover, compared to a pore-throat or fracture network created using synthetic materials, Nooraiepour et al. (2018) used a natural organic-rich shale sample to create a fracture network through laser scribing on the sample surface. They aimed to ensure a similar wettability and surface free energy between experimental substrates and real rocks, which may influence the nucleation and precipitation of salt crystals.

On the other hand, unlike the core-flooding system, which uses brine with typical salt components to enhance the X-ray contrast between salt and CO_2, the microfluidic-chip system generally uses different additives into synthetic brine. These include insoluble dye particles (Miri et al., 2015), potassium permanganate dye (Ho and Tsai, 2020), or low-concentration fluorescein (Kim et al., 2013; Rufai and Crawshaw, 2017, 2018). During the microfluidic-flooding experiment, the processes of water evaporation and salt precipitation can be observed in real-time through the transparent chips. Meanwhile, these brine additives enable better visualization under polarizing light or fluorescence microscopy. The microscopy system can capture real-time images at short time intervals to record the whole process of chip dry-out. Furthermore, the images can be used to extract quantitative kinetic data of evaporation and precipitation using image processing tools, such as ImageJ (Kim et al., 2013; Rufai and Crawshaw, 2017, 2018).

2.3 Static batch and surface drying experiment systems

In the context of CGS, the static batch experiment system is generally used for fluid-rock interaction studies (Kaszuba et al., 2013). However, several peer-reviewed publications documented the phenomenon of salt precipitation in their batch experiments (e.g., Bolourinejad and Herber, 2013; Rathnaweera et al., 2016; Wang et al., 2016; Dai et al., 2022; Md Yusof et al., 2022). Some of these experiments presented useful evidence for the elucidation of the influencing factors of salt precipitation. For instance, Wang et al. (2016) and Bolourinejad and Herber (2013) discussed the effect of gas impurity during CO_2 injection on salt precipitation. Compared to the dynamic core-flooding and microfluidic-chip experimental systems with continuous fluid flooding, the static batch experiment system features a closed reaction system, where no significant materials are introduced or removed during the reaction process. The main apparatus for the batch experiment is a high-temperature and high-pressure reactor that contains rock specimens (rock powders, disks or cores), brines, and injected CO_2. A detailed description of experimental apparatuses for CO_2-brine-rock interactions can be found in the review article by Kaszuba et al. (2013). Unlike water evaporation and salt precipitation, which occur very rapidly, dissolution and precipitation of major rock-forming minerals happen at very slow rates, with the exception of carbonate minerals (Black et al., 2015; Holzheid, 2016). Thus, the duration of a batch experiment is relatively long, ranging from several weeks to years. For instance, Rathnaweera et al. (2017) carried out a static experiment to capture the initial dissolution of quartz and aluminosilicate minerals that lasted 1.5 years.

Compared to the dynamic flooding and the static batch experiments, the surface drying experimental system can be regarded as a semi-dynamic to semi-static experiment. This approach generally follows a simple procedure, including core evacuation, brine saturation, and drying in an oven or by surface air blowing. This means that the specimen is not subjected to gas flooding during water evaporation and salt precipitation. However, the residual brine must have experienced capillary convection due to the fluid saturation difference between the drying surface and the specimen interior. To date, several studies have

documented salt precipitation using the drying oven experiment (e.g., Peysson et al., 2011a; Tang et al., 2015; Bernachot et al., 2017; Zhang et al., 2020). This kind of experiment is generally used to study plants and soils, land-atmosphere interactions, and buildings and monuments. However, some surface drying experiments also presented useful clues to reveal the influencing factors of salt precipitation. For instance, Norouzi Rad and Shokri (2014) and Norouzi Rad et al. (2015) elucidated the effects of pore and particle geometry characteristics on salt precipitation. Compared to the dynamic flooding experiment that simulates CO_2 injection and salt precipitation in the main reservoir body, the surface drying experiment can be used to study the salt precipitation at specific interfaces, such as the contact interface between reservoir and caprock, high-permeability layer and low-permeability layer, or open fracture and low-permeable matrix.

3 Distribution patterns of salt precipitation

As summarized in the review article by Miri and Hellevang (2016), salt precipitation during CO_2 injection is the consequence of a series of physical processes with minor chemical processes. These processes mainly include two-phase displacement of brine by viscous pressure gradients imposed by injected CO_2, evaporation of brine in contact with unsaturated CO_2 stream, backflow of brine to evaporation front driven by capillary pressure gradient, molecular diffusion of salt solute due to concentration gradient, salt nucleation and growth from supersaturated brine, and salt self-enhancement mechanisms. Readers can refer to the previous review article for detailed descriptions of salt precipitation processes (Miri and Hellevang, 2016). The interplay of these mechanisms determines the macro-distribution at the reservoir scale and the micro-distribution at the pore scale of salt precipitation and thus the resulting reservoir impairment. This section aims to provide a general overview of the distribution patterns of salt precipitation, and to improve our understanding by reviewing recently published articles.

3.1 Macro-distribution of salt precipitation

As proposed by Ott et al. (2015) and Miri and Hellevang (2016), the macro-distribution patterns of salt precipitation at the reservoir scale are controlled by three drying regimes, namely the diffusive, capillary, and evaporation regimes. The diffusive regime dominates under the conditions of low injection and evaporation rates. In this case, the capillary backflow of brine can compensate for the water loss due to evaporation near the injection point. Meanwhile, the salt solutes have enough time to diffuse away from the injection point under salt concentration differences. This results in a semi-homogeneous distribution of salt precipitation near the injection well. The capillary regime is active under the conditions of moderate injection rates and during the equilibrium between evaporation rates and capillary backflow rates. A drying front forms and moves away from the injection point, and then stabilizes at a position where the capillary backflow rate equals the evaporation rate. Therefore, a locally intensive salt precipitation belt forms near the drying front because there is not enough time for the homogenization of the salt solutes via diffusion. The evaporative regime forms at very high injection rates, above a critical limit. In this case, the evaporation rate is constantly greater than the capillary backflow rate, and the drying front constantly advances through the reservoir. This results in a homogeneous salt distribution due to the lack of sufficient capillary backflow of brine.

Several experimental studies have verified the different salt distribution patterns (e.g., Ott et al., 2011, 2015; Falcon-Suarez et al., 2020; Mascle et al., 2023). Locally intensive salt precipitation in the capillary regime is responsible for the reservoir injectivity impairment during CO_2 injection. The continuous

capillary backflow of brine towards the drying front must simultaneously meet the following requirements, including adequate ex-situ brine sources and connected brine migration pathways. The ex-situ brines for local salt precipitation are not only sourced from lateral reservoirs but also adjacent low-permeability interlayers (Roels et al., 2016; Lopez et al., 2020). The connected brine migration pathways associated with capillary backflow consist of wetting films on grain surfaces, liquid bridges, and liquid pools (Miri et al., 2015). As pointed out by experimental studies (Ott et al., 2013, 2021; Rufai and Crawshaw, 2018; He et al., 2019, 2022; Akindipe et al., 2022), residual brine saturation and rock wettability are critical factors influencing the liquid migration pathways. Low residual brine saturation or hydrophobic wettability can reduce hydraulic connectivity and thus prevent brine migration. The ex-situ brine sources and brine migration pathways for salt precipitation are further discussed in sections 4.1 Brine aspect and 4.2 Rock aspect.

3.2 Micro-distribution of salt precipitation

Two main types of salt crystal morphologies were identified in the experiments of Kim et al. (2013) and Miri et al. (2015), namely large bulk salt crystals and polycrystalline salt aggregates (Fig. 1). Subsequently, further experimental studies confirmed the previous findings of crystal characteristics (He et al., 2019, 2022; Ho and Tsai, 2020). Large bulk salt crystals tend to form when single crystals nucleate close to the CO_2-brine interfaces at low supersaturations. Salt crystals have enough time to grow and attain large sizes, especially at low evaporation rates. In contrast, micro polycrystalline aggregates tend to form at the CO_2-brine interfaces of high supersaturations. Salt crystals feature small sizes and fast nucleation and precipitation rates due to high evaporation rates (Fig. 1). Kim et al. (2013) and Miri et al. (2015) documented that large bulk crystals mainly form in the early stage of CO_2 injection when sufficient brines are available, while micro polycrystalline aggregates mainly occur later at CO_2-brine interfaces when brines diminish due to two-phase displacement and continuous evaporation. However, Ho and Tsai (2020) noted that the two salt morphologies can occur at different stages of salt precipitation, although the specific characteristics of each type vary slightly between stages.

Apart from the macro-distribution of salt precipitation, the micro-distribution of salt crystals is also considered a direct factor controlling reservoir permeability impairment. However, there is still some debate regarding the micro-distribution of salt crystals. Firstly, it is controversial whether salt crystals are mainly distributed in small or large pore throats. Tang et al. (2015) found that salts precipitate in all pore-throat sizes in certain experiments, although some of their experiments showed salts concentrating primarily in small pore throats. However, Tang et al. (2023) compared pore-throat sizes from NMR tests before and after drying in their later experiments, and observed that more salts precipitate in large pores. Zhang et al. (2020) observed that the average pore-throat size significantly decreases when comparing mercury intrusion curves before and after drying, and claimed that large pore throats can be divided into smaller ones due to salt precipitation. Ott et al. (2014) studied salt precipitation in dual-porosity systems. They found that salts can precipitate in the micro-pores when the flowing CO_2 in the macro-pores reaches the interface between macro- and micro-pores. Otherwise, salt precipitation may concentrate in the macro-pore system while the micro-pore system acts as the brine source of capillary backflow. Overall, the differences in the micro-distribution pattern of salt precipitation derived from various experimental studies could be due to the different assemblages of pore structures and injection characteristics. In a heterogeneous pore structure, the injected CO_2 always migrates along the connected large pore-throats at relatively low injection pressures, and the salts tend to concentrate in the pore-throats of the preferential migration pathways. At higher injection pressures, the injected CO_2 reaches more pore-throats with various

sizes, and therefore the salts could precipitate in pore-throats of a wide range of sizes.

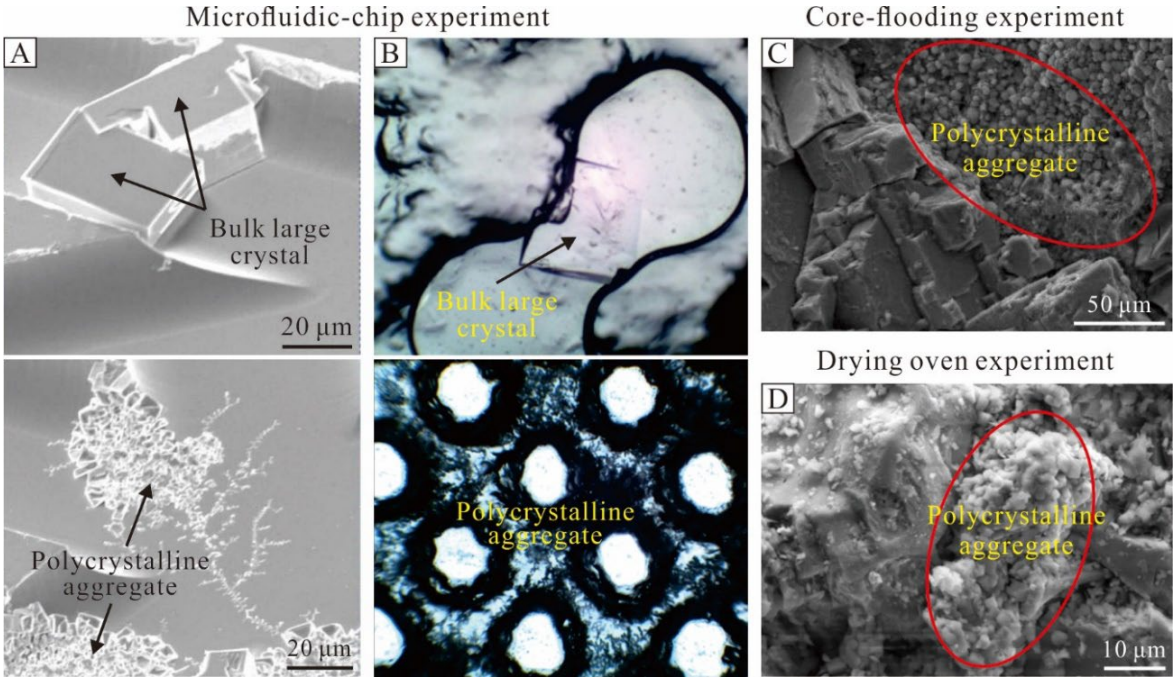

Fig. 1. Two main types of salt crystal morphologies, namely large bulk salt crystals and polycrystalline salt aggregates, revealed by (A-B) microfluidic-chip experiment (Kim et al., 2013; Miri et al., 2015), (C) core-flooding experiment (Tang et al., 2023), and (D) drying oven experiment from the authors of this article.

Secondly, there is an argument about whether salt crystals are able to penetrate the CO_2-brine interfaces. Miri et al. (2015) proposed that the salt self-enhancement mechanism can promote the growth of salt aggregates into the gas phase. The micro-pore structures and significant hydrophilicity of salt aggregates result in strong capillary suction to ex-situ brine. Furthermore, the salt aggregates enhance the evaporation surfaces and nucleation sites. Therefore, the salt self-enhancement mechanism can lead to more salt precipitation at higher rates, which in turn can significantly block CO_2 seepage pathways. Masoudi et al. (2021) implemented a pore-scale simulation of the salt self-enhancement process using an advection-diffusion Lattice-Boltzmann model, considering both intergranular pores of reservoirs and intercrystalline pores of salts. In contrast, Ott et al. (2011, 2015) claimed that salt precipitation primarily occurs in the pore spaces that were previously occupied by residual brines. They highlighted that the benefits of brine evaporation on the relative permeability of CO_2 are more significant than the drawbacks of salt blockage. Intensive salt precipitation may only reduce the effective permeability of CO_2 in heterogeneous multi-porosity systems where micro-pores provide brine for evaporation and salt precipitation in macro-pores (Ott et al., 2013, 2014). We believe that the absence of salt precipitation in the CO_2 flow channels in some of the experiments may be due to the limitations of experimental samples and conditions. The small sample size and high sample permeability and injection rate result in salt precipitation relying only on in-situ residual brine, which is inconsistent with the potential backflow of peripheral brine in subsurface reservoirs and may underestimate the salt precipitation in real reservoirs. However, as pointed out by Ott et al. (2021), the salt self-enhancement mechanism to explain how salt precipitation penetrates the CO_2-brine interfaces has only been observed in microfluidic experiments, and it has not yet been proven in core-flooding experiments using rock samples.

4 Comprehensive analysis of controlling factors

Although salt precipitation follows the same basic principles in different experiments, these experiments can yield inconsistent or even conflicting conclusions. This is because the complex processes of salt precipitation, the macro and micro distributions of salts, and their effects on reservoir physical properties may vary from core to core or from site to site. Therefore, this section aims to provide a critical review of various controlling factors on salt precipitation. These factors have been categorized into four distinct groups, namely the brine, rock, gas, and injection scenario aspects.

4.1 Brine aspect

4.1.1 Brine salinity

Brine salinity is generally considered as the main factor controlling the process of salt precipitation during gas production and storage. A larger number of experiments have been conducted to elucidate the effects of brine salinity on water evaporation, salt precipitation, and the variation of reservoir properties, using the core-flooding system (Peysson et al., 2011b, 2014; Peysson, 2012; Jeddizahed and Rostami, 2016; Sokama-Neuyam and Ursin, 2018; Sokama-Neuyam et al., 2023, 2019; Jayasekara et al., 2020; Md Yusof et al., 2020; Abbasi et al., 2022; Edem et al., 2022; Tang et al., 2023), the microfluidic-chip system (Rufai and Crawshaw, 2017, 2018; Seo et al., 2019; He et al., 2022), and the drying oven system (Peysson et al., 2011a; Tang et al., 2015). In addition, many numerical simulation studies have also been performed to verify the effects of brine salinity (Kim et al., 2012; André et al., 2014; Cui et al., 2016, 2018a; Ghafoori et al., 2017; Wang et al., 2017; Kumar et al., 2020; Parvin et al., 2020; Norouzi et al., 2021; Ren and Feng, 2021; Zhao and Cheng, 2022).

Brine salinity ranging from near zero to full saturation is used in various experiments, and determines the amount of salt available for precipitation per unit of brine. Higher salinity leads to increased salt precipitation and hence increased impairment of absolute permeability, as shown in all the aforementioned experimental and numerical studies, e.g., Fig. 2A. However, effective permeability is determined by both absolute permeability and relative permeability. Peysson (2012) carried out a series of core-flooding experiments using different concentrations of KCl solution. Although salt precipitation leads to a reduction in absolute permeability even at low salt concentrations, effective permeability improves due to the increase in the relative permeability of CO_2. This is because water evaporation into the undersaturated CO_2 stream expands the pathways for CO_2 migration. However, as the initial brine salinity increases, the effective permeability initially increases at the early evaporation stage, but subsequently falls significantly with intensive salt precipitation (Peysson, 2012). Thus, water evaporation and salt precipitation have opposite effects and together determine the final effective permeability variation for CO_2 migration. Tang et al. (2023) conducted a series of core-flooding experiments to simulate the drying process during underground CH_4 storage at the initial residual brine saturations ranging from 30% to 50%. They concluded that the effective porosity and permeability are higher than the initial values in all experiments using different brine salinities, but the improvement diminishes with increasing salinities. In other words, the positive effect of water evaporation outweighs the negative effect of salt precipitation in their study.

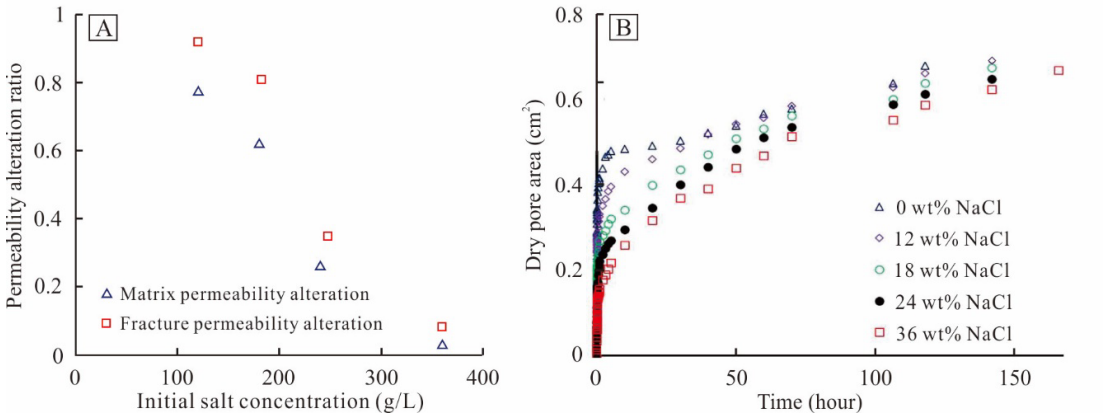

Fig. 2. Effect of initial brine salinity on (A) permeability alteration (the ratio of current absolute permeability to initial absolute permeability) and (B) evaporation rate, indicating that higher initial brine salinity results in greater permeability impairment and lower evaporation rate, modified from Rufai and Crawshaw (2017).

Salinity not only determines the amount of salt precipitation, but also influences the processes of brine evaporation and salt crystallization. Seo et al. (2019) documented a trend in the average evaporation rate, which first decreases and then increases as the initial salinity rises, with the lowest rate occurring at the initial NaCl concentration of 5%-10%. They attributed this to the corresponding variation of the activity coefficient of NaCl solution, with salinity controlling brine evaporation dynamics. As the activity coefficient decreases, the energy required to separate the constituent molecules increases. This means that the diffusion of water molecules from liquid brine to gaseous CO_2 is more challenging at lower water activities. On the other hand, Jeddizahed and Rostami (2016) documented a decreasing evaporation rate as the initial salinity increases from 5 g/L to 200 g/L. They explained that higher salinity leads to a higher viscosity difference between CO_2 and brine, a lower displacement efficiency, and thus a higher amount of residual brine. Therefore, there is an increasing chance of brine getting in contact with CO_2 and evaporating. However, higher salinity leads to a lower equilibrium vapor pressure and thus a lower evaporation rate. Ultimately, the negative effect of salinity on equilibrium vapor pressure overcomes the positive effect on residual brine saturation. Similarly, Abbasi et al. (2022) reported that high salinity leads to weaker evaporation due to the decreasing equilibrium vapor pressure according to Raoult's law. Rufai and Crawshaw (2017) and Jayasekara et al. (2020) found that more salt precipitation in high salinity impairs evaporation rate by blocking the paths of CO_2 migration and brine backflow (Fig. 2B). High salinity implies high viscosity and low mobility of brine, which may hinder the backflow of brine to the evaporation front (Rufai and Crawshaw, 2017). In contrast, Peysson et al. (2011b) found that evaporation rate is higher at salinities of 250 or 300 g/L than 30 g/L. They claimed that salt efflorescence forms on the specimen surface under the condition of high salinity brine, and the microporous structure of the efflorescence enhances the capillary backflow of brine from the sample interior to the evaporation surface. This phenomenon has been found in the surface drying cases by Sghaier and Prat (2009). Overall, the effect of brine salinity on evaporation rate is the coupling of several opposing factors. Positive effects include higher residual brine saturation and increasing brine backflow due to microporous salts. Negative effects include lower equilibrium vapor pressure and blockage of CO_2 migration pathways. Thus, the final evaporation rate of brine varies from case to case due to the different combinations of the above positive and negative effects. Although there is still ongoing debate about the effect of salinity on evaporate rate, an increase in brine salinity increases the total dissolved solids per unit of brine. The effect of salinity on precipitation rate is controlled by the interaction between the change in evaporation rate and the increase in total dissolved solids (Jeddizahed and Rostami, 2016; Abbasi et al., 2022).

4.1.2 Brine composition

Most studies used NaCl solution as the experimental fluid due to its simplicity and because it is the main component of most subsurface brines. As mentioned in the experimental methodology section, some experiments adopted Br/I or Cs salts instead of Cl salts to improve the X-ray contrast between CO_2 and brine/salt (e.g., Van Hemert et al., 2013; Ott et al., 2014, 2015, Roels et al., 2014, 2016, Akindipe et al., 2021, 2022; Mascle et al., 2023). Furthermore, several experiments used K salts rather than Na salts, as the former not only have higher density and X-ray attenuation, but also a lower critical salt concentration and are therefore easier to precipitate (Peysson, 2012; Ott et al., 2014; Peysson et al., 2014; Roels et al., 2014, 2016; Lopez et al., 2020). In addition, many experiments used underground brines or synthetic brines according to the composition of real brines (e.g., Bolourinejad and Herber, 2013; Golghanddashti et al., 2013; Tang et al., 2015, 2023; Sokama-Neuyam et al., 2019; Wang et al., 2019; Abbasi et al., 2022). However, there are very few studies that have addressed the issue of the effect of brine composition on salt precipitation during gas storage. Peysson et al. (2011a) compared the experimental results using different brine compositions. Their study showed that KCl solution results in a more significant permeability impairment of rock cores. Edem et al. (2022) carried out a series of experiments using four different types of brines, uniquely composed of NaCl, KCl, $MgCl_2$, and $CaCl_2$. Although they found complex relations between porosity and permeability reductions and salt types (Fig.3), they pointed out that aquifers with high proportions of divalent salts, especially magnesium salts, tend to undergo more intense salt precipitation and injectivity impairment. In addition, both experimental and numerical simulation studies indicated that CO_2 solubility in divalent solutions is noticeably lower than that of monovalent solutions (Tsai et al., 2015; Messabeb et al., 2017). Therefore, there is more CO_2 in the free phase, resulting in faster water evaporation and salt precipitation in divalent brines. To the best of our knowledge, the studies of gypsum or aragonite precipitation during evaporation experiments in the context of CO_2 storage are extremely rare. This may require further studies, as aragonite and gypsum may have different crystallization habits to other salts, and may impair permeability stronger at lower porosity changes.

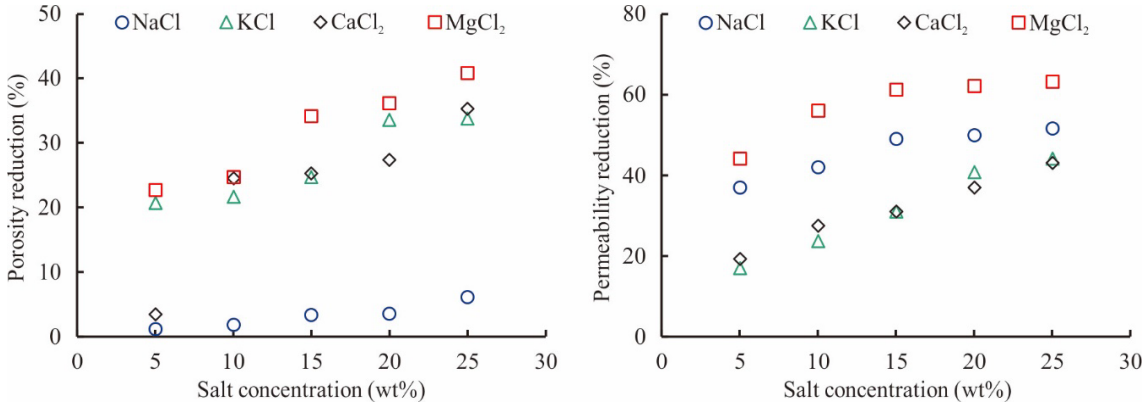

Fig. 3. Effect of brine composition on porosity and permeability alternation, indicating that high proportions of magnesium salts lead to more intense salt precipitation and hence higher porosity and permeability reduction, data from Edem et al. (2022).

4.1.3 Brine source

In-situ brine saturation of reservoirs varies from 100% in aquifers to irreducible water saturation in hydrocarbon reservoirs. Brine saturation determines the amount of brine involved in two-phase displacement, water evaporation, and salt precipitation. Most studies have used fully brine-saturated cores or chips in their drying experiments, while a few studies have investigated the effects of initial brine

saturations on salt precipitation. For instance, Zhang et al. (2020) carried out a series of drying-oven experiments with increasing initial brine saturations. They found that porosity and permeability impairment increase significantly with initial brine saturation increasing from 10% to 100% (Fig. 4). Ott et al. (2013, 2021) compared three core-flooding experiments with different saturation conditions. The 100% initial brine saturation scenario (≈50-60% after two-phase displacement) and the remaining brine saturation (≈50%) scenario, obtained by draining the fully brine-saturated core with decane, present significant reductions in permeability after drying by CO_2 flooding. However, the residual brine saturation scenario (12-23%), obtained by centrifugation followed by decane drainage, features a minor change in effective permeability. This is because there is limited brine available for evaporation and salt precipitation in the last scenario, and it is mainly concentrated in small pore throats. Moreover, it is difficult to form the effective capillary flow of residual brine and the local enrichment of salt precipitation due to the lack of hydraulic connectivity. Meanwhile, the effects of brine saturation on salt precipitation have also been confirmed by numerical simulations (e.g., Kim et al., 2011; Wang and Liu, 2013; Cui et al., 2016, 2021). Cui et al. (2016, 2021) simulated CO_2 geothermal exploitation in depleted gas reservoirs, and reported that less salt precipitation and permeability impairment occur when the injection and production wells are placed in the upper position of the gas reservoirs. This is because that there is lower residual brine saturation in the upper part of the reservoirs than in the lower part.

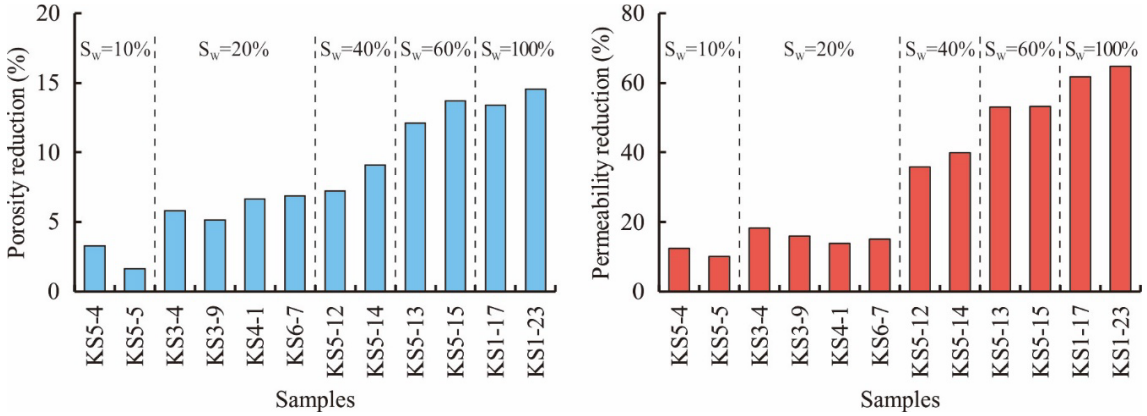

Fig. 4. Effect of initial brine saturation (S_w) on porosity and permeability alternation, indicating that higher initial brine saturation leads to higher porosity and permeability reductions, data from Zhang et al. (2020).

Apart from the in-situ brines, the ex-situ brines driven by capillary backflow are an important source of evaporative salt precipitation, such as the brine supply from matrix to fracture, from weak-permeable interlayer to reservoir, and from the interior of the reservoir. The first two scenarios result from the reservoir heterogeneity at different scales, and are discussed in detail in Section 4.2 the rock aspect. Regarding the capillary backflow due to the brine saturation gradient within the reservoir, Baumann et al. (2014) found that the salt saturation in the dry-out region increases from the center area to the edge area, based on the time-lapse radiometric pulsed neutron-gamma logging data of the injection well at the Ketzin CO_2 storage site. They explained the salt distribution pattern as the presence of large capillary forces leading to the backflow of additional brine at the dry-out edges. Moreover, Grude et al. (2014) found that the permeability reduction of core plugs due to salt precipitation from laboratory experiments is 7% (horizontal core plug) and 17% (vertical core plug). However, the experimental results are not sufficient to explain the significant pressure build-up due to near-well plugging from field data of the Snøhvit storage site. As pointed out in the core-scale numerical study by Ren et al. (2018), the core sizes used in core-flooding experiments are limited by the experimental apparatus used. Thus, the amount of brine available for capillary backflow is limited by the short core sizes, which may cause a significant underestimation of

the amount of local salt precipitation. Although several studies have used cores longer than 20 cm (e.g., Muller et al., 2009; Wang et al., 2009, 2010, Sokama-Neuyam et al., 2017a, 2019; Berntsen et al., 2019), it is still unknown whether these sizes are large enough to mimic reservoir conditions, as the effective backflow distance of brine is vague.

To avoid the problem of limited brine replenishment, Berntsen et al. designed a medium-scale borehole physical model (20 cm × 19 cm) with an infinite source of formation water (Berntsen et al., 2019). Infinite brine replenishment was achieved by radial injection of brine into the vicinity of the borehole at the same rate as water evaporation. They explained that the overall weak salt precipitation, concentrated in the CO_2 inlet, results from the constant backflow of brine. This delays the oversaturation of brine, and requires more experimental time to achieve significant salt precipitation. Lopez et al. (2020) and Mascle et al. (2023) designed a simultaneous CO_2 and brine injection experiment program. CO_2 and brine were injected from the top and bottom inlets, respectively, while all fluids flowed out through the bottom outlet (Fig. 5). This allowed the simultaneous flooding of CO_2 throughout the whole core sample and brine flooding at the bottom face of the core sample. The latter can provide a brine source for the backflow towards the evaporation front. The infinite brine source not only increases the amount of salt precipitation, but also changes the salt formation process and distribution pattern. They observed the movement and growth of local salt banks due to the repeated dissolution and precipitation of salts during gas draw-down to build-up cycles. The replenishing brine dissolves the rear back of the first salt bank, and the dissolved salts move upwards and precipitate to form the second salt bank (Fig. 5).

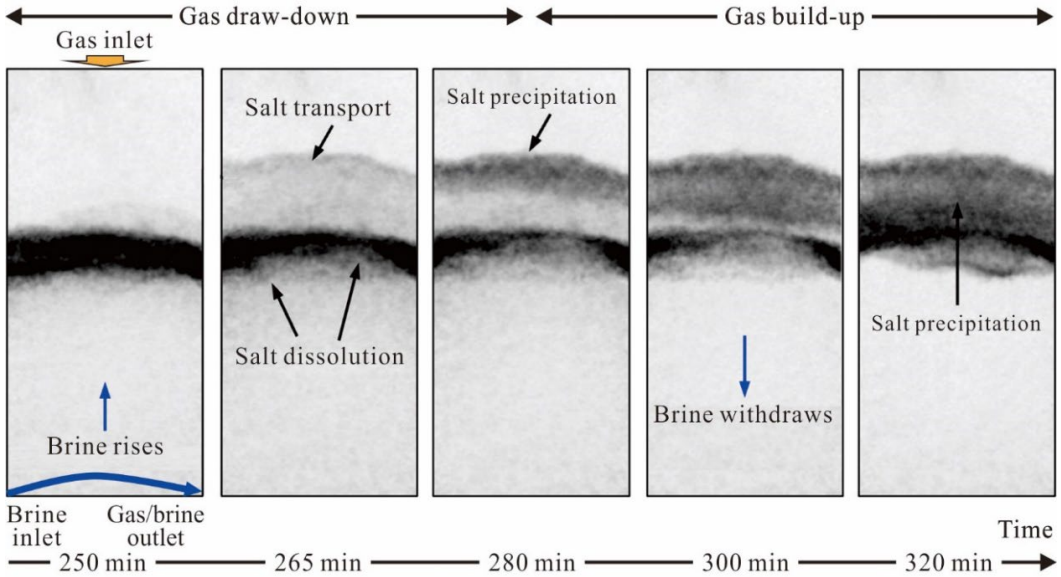

Fig. 5. Effect of significant brine replenishment on salt precipitation, indicating that the replenishing brine increases the amount of salt precipitation and leads to the movement and growth of salt banks due to salt dissolution and reprecipitation during a gas draw down to build up cycle, modified from Mascle et al. (2023).

4.2 Rock aspect

4.2.1 Initial porosity and permeability

Although potential storage reservoirs generally have high initial porosity and permeability, some storage sites with inferior properties have to be used due to other considerations. Several experimental studies have investigated the effect of initial reservoir properties on salt precipitation and permeability impairment (e.g., Vanorio et al., 2011; Bacci et al., 2013; Golghanddashti et al., 2013; Peysson et al., 2014; Tang et al.,

2015, 2023; Ho and Tsai, 2020; Md Yusof et al., 2020; Abbasi et al., 2022). Most studies concluded that low-permeability reservoirs tend to suffer more from higher permeability impairment caused by salt precipitation. These experimental findings are consistent with the field observations at the injection well of the Boundary Dam storage project (Talman et al., 2020). They found that the most extensive salt precipitation occurs in the least permeable reservoir interval, and the precipitated salts in the high-permeability reservoir interval concentrate in the less permeable part of the perforated zone. Compared to high permeability reservoirs, low-permeability reservoirs are characterized by higher in-situ residual brine saturations after two-phase displacement, lower CO_2 injection rates at the same injection pressure, and higher potential for capillary ex-suit brine transport (Peysson et al., 2014). Thus, more in-situ and ex-situ brine is available for local salt precipitation in low-permeability reservoirs, resulting in greater injectivity impairment (Fig.6; Golghanddashti et al., 2013). In addition, low permeability generally means small pore-throat size and high pore-throat tortuosity, therefore these reservoirs are more sensitive to salt precipitation blockage (Tang et al., 2015).

Some numerical simulation studies have also discussed the effect of the initial porosity and permeability on salt precipitation pattern and reservoir impairment through sensitivity analyses (e.g., Kim et al., 2012; Wang and Liu, 2013; Cui et al., 2016, 2018a; Ghafoori et al., 2017; Norouzi et al., 2021; Zhao and Cheng, 2022). Several studies concluded that increasing the initial porosity and permeability alone plays a very weak role in reducing reservoir impairment, and can even promote salt precipitation in some cases (Wang and Liu, 2013; Cui et al., 2016; Ghafoori et al., 2017; Norouzi et al., 2021). These numerical simulation results are inconsistent with the above experimental results. This is mainly because only permeability and porosity were changed, while other parameters were kept constant during these numerical sensitive analyses. In other words, these studies did not consider the fact that porosity and permeability changes should be accompanied by changes in a series of key parameters, such as residual brine saturation, capillary pressure curve, and relative permeability curve. This type of inconsistency between numerical and experimental studies also exists in the analyses of many other controlling factors of salt precipitation. Therefore, the key is to find the intrinsic relationship and interaction of these factors, and then to incorporate them into numerical simulations.

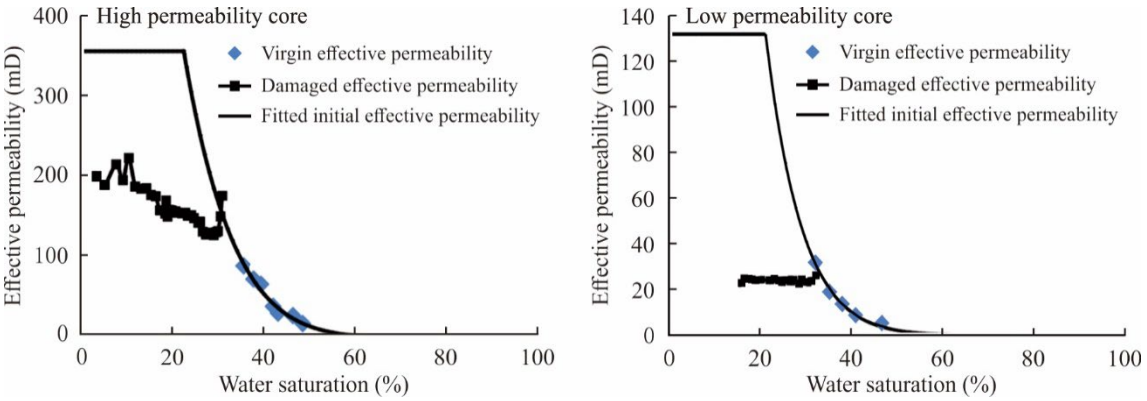

Fig. 6. Effect of initial reservoir permeability on permeability alternation caused by salt precipitation, indicating that lower initial permeability tends to feature higher permeability impairment, modified from Golghanddashti et al. (2013).

4.2.2 Reservoir heterogeneity

4.2.2.1 Heterogeneous pore structure at the micro-scale

The size, sorting and connectivity of pore throats exert significant effects on the migration and distribution of brine and CO_2, which in turn controls salt precipitation. Several core-flooding experiments have been conducted to compare the drying in sandstones and carbonates (Bacci et al., 2013; Ott et al., 2013, 2014, Akindipe et al., 2021, 2022). These two rocks have different wettability and pore structure characteristics. Sandstones, especially well-sorted ones, are less heterogeneous than carbonates concerning pore structure. Carbonates tend to feature lower permeability than sandstones for the same given porosity, due to their multiple pore-throat sizes and high pore-throat tortuosity. Thus, during CO_2 injection, carbonates have higher residual brine saturation for salt precipitation and are more sensitive to reservoir damage (Bacci et al., 2013). Akindipe et al. (2021, 2022) pointed out that salt precipitation is faster in sandstones, but ends earlier. This is due to the higher evaporation rates resulting from higher CO_2 flow velocities. Moreover, most salts occupy the corners of scCO_2-filled pores in sandstones, and these pore corners are previously filled by residual brine (Fig. 7A). In contrast, multi-porosity carbonates suffer from more and longer salt precipitation. In addition to the salts located in the pore corners, many salts completely block pores ranging from small to large sizes (Fig. 7B), resulting in severe permeability impairment in carbonates. Ott et al. (2013, 2014) explained that the micro-porous volume acts as a brine and salt supplier to the CO_2-conducting macro-porous volume in the multi-porosity carbonates. Although, the brine and salt transport between micro- and macro-pores is a dynamic and complex process (Ott et al., 2014), overall, the development of heterogeneous multi-porosity leads to enhanced reservoir damage by salt precipitation. In the experiments of Tang et al. (2023), dual-porosity sandstones present a significant reduction in the size of large pores, while the small pores are largely unaffected. All these studies indicate that operating CO_2 storage in a relatively homogeneous reservoir is favorable to avoid severe injectivity impairment.

Some potential storage sites are located in fractured reservoirs, where the enhanced permeability due to fractures (secondary permeability) surpasses that of other pore types. Several core-flooding and micro-chip experiments have been used to study the drying in a pore-facture system (e.g., Miri et al., 2015; Nooraiepour et al., 2018; Lima et al., 2021; He et al., 2023). Matrix pore throats can act as a brine source to provide water and salt for the evaporation and precipitation in fractures. With the gradual blockage of fractures, CO_2 can start to invade the matrix pore throat system leading to salt precipitation there (Miri et al., 2015; He et al., 2023). Thus, salt precipitation can cause severe permeability damage in both fractures and matrix pores. For fractured caprocks, Nooraiepour et al. (2018) reported that the extensive salt precipitation in fractures can be considered as a fracture healing mechanism that reduces the risk of CO_2 leakage. Norouzi Rad and Shokri (2014) and Norouzi Rad et al. (2015) conducted a series of surface drying experiments using packed columns formed by glass beads and quartz sands of different sizes. These surface drying experiments indicate that the column can provide a brine source for evaporation and precipitation near the column surfaces, which is similar to the drying process in the fracture-matrix system. These studies revealed that grain angularity, size and sorting determine the morphology, size and connectivity of matrix pore throats, and thus control the capillary backflow of brine to the drying surface and the invasion of gas into matrix. In addition, a few numerical simulation studies have also found that the salt precipitation in fractures or on surfaces is significantly affected by the matrix properties (Nachshon et al., 2011; Dashtian et al., 2018; Sokama-Neuyam et al., 2020). The fractures or surfaces suffer from more severe blockage by salt precipitation, while the matrix has more residual brine and more interconnected pathways of brine backflow.

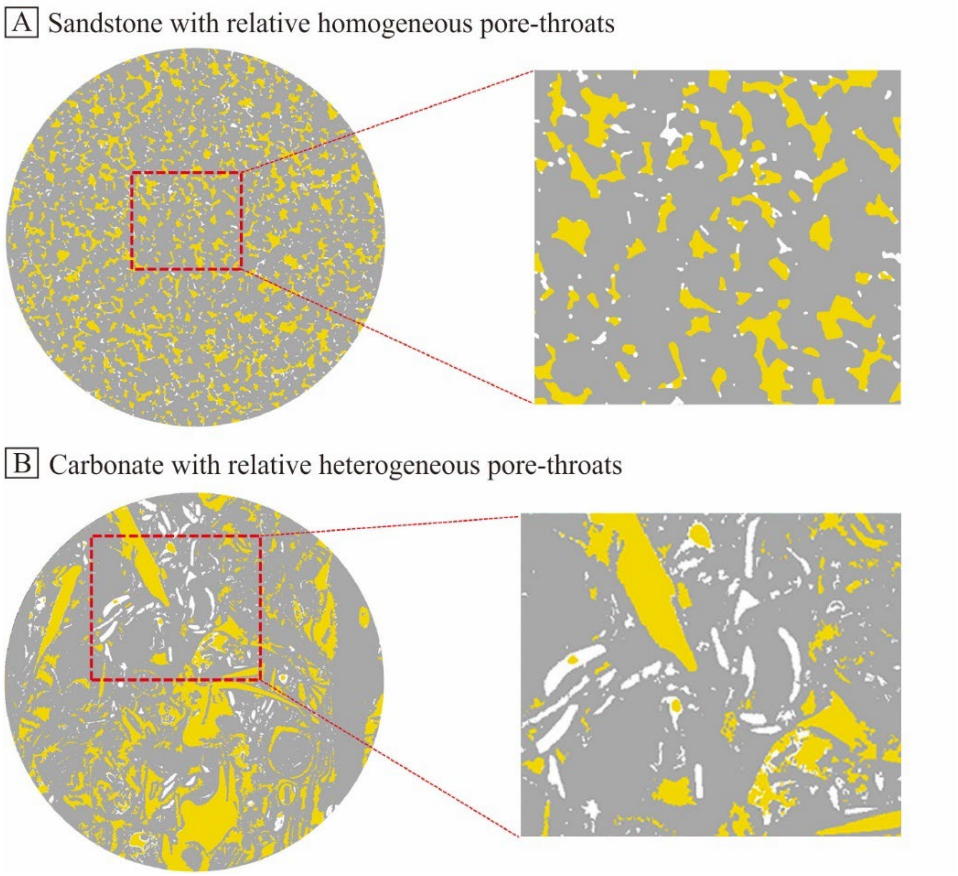

Fig. 7. Effect of pore-throat heterogeneity on salt distribution (color scheme: CO_2=yellow; salt=white; grain=gray): (A) less salts in homogeneous sandstone concentrate in the corners of scCO_2-filled pores and (B) more salts in heterogeneous carbonate block the pores ranging from small to large sizes, modified from Akindipe et al. (2021).

4.2.2.2 Heterogeneous reservoir structure at the macro-scale

The heterogeneous reservoir structure at the macro-scale also exerts significant effects on drying due to brine transport from low-permeability layers to high-permeability layers. Roels et al. (2016) and Lopez et al. (2020) manufactured layered core samples by assembling high- and low-permeability cores. This study aimed at mimicking the capillary contact between the high-permeability reservoir and the low-permeability interlayer. The injected CO_2 mainly invades the high-permeability reservoir, while the residual brine in the low-permeability interlayer can be transported into the adjacent reservoir by capillary force with continuous drying in the reservoir. The presence of low-permeability interlayers not only increases the amount of salt precipitation in the adjacent reservoirs, but also changes the salt distribution patterns. For instance, Lopez et al. (2020) found that a salt bank lies in diagonal to the high-permeability Bentheimer sandstone due to the interplay of the lateral and vertical brine supply (Fig. 8). Grude et al. (2014) argued that one of the reasons why experimentally obtained permeability impairments are much lower than filed data of the Snøhvit storage site may lie in the failure of the core-scale experiment to capture reservoir-scale heterogeneity.

Compared to the limited number of experimental studies, a greater number of numerical simulation studies focus on the effect of heterogeneous reservoir structures on drying or on the drying at the reservoir-caprock interface (e.g., Qi et al., 2009; Chasset et al., 2011; Kim et al., 2014; Ren et al., 2018, 2022; Zhao and Cheng, 2022). This is because constructing complex heterogeneous reservoir models is much easier with numerical methods than with experimentally. From one of these numerical modeling studies, Ren et

al. (2022) concluded that the dry-out effect can be significantly underestimated when a completely heterogeneous model is simplified to a deterministic multi-facies heterogeneous model. Apart from the sand-mud interbedded reservoir structure, a few numerical studies have discussed the effect of permeability anisotropy on drying (Guyant et al., 2015; Cui et al., 2018b). Vertical permeability is generally lower than horizontal permeability, especially in stratified rocks. They found that increasing the ratio of horizontal to vertical permeability promotes the lateral migration of CO_2, which inhibits the lateral capillary backflow of brine and the local accumulation of salts.

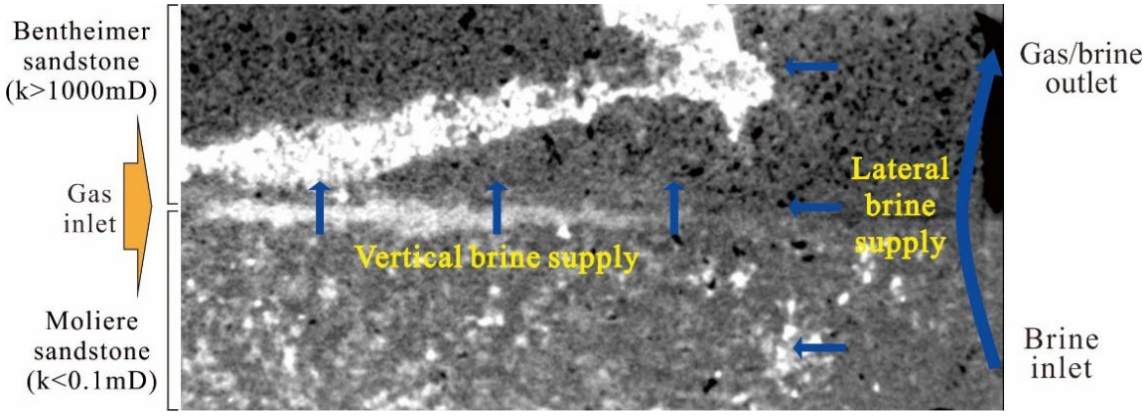

Fig. 8. Effect of reservoir structure with low-permeability interlayers on salt precipitation (Bright zone corresponds to solid salts), indicating that an additional salt bank forms in the diagonal of the high-permeability sandstone due to the interplay of the lateral and vertical brine supply, modified from Lopez et al. (2020).

4.2.3 Rock wettability

Although most clastic saline aquifers are water-wet, hydrocarbon reservoirs available for CO_2 storage are likely to have variable wettability. Rock wettability exerts significant effects on fluid migration and distribution, and hence salt precipitation. A few core-flooding and micro-chip experiments have focused on the wettability effects (e.g., Rufai and Crawshaw, 2018; He et al., 2019, 2022; Akindipe et al., 2022). He et al. (2019, 2022) obtained hydrophilic, neutral and hydrophobic micro-chips using a freshly fabricated micromodel, a chip cleaned after the initial drying test, and a chip processed in a furnace at high temperature, respectively. Rufai and Crawshaw (2018) obtained mixed wettability and oil wettability micro-chips by the flooding of dodecane containing dissolved silicon caulk into a water-saturated micromodel and a dry micromodel, respectively. In the core-flooding experiment, Akindipe et al. (2022) obtained hydrophobic core samples by oil displacement of water-saturated cores followed by water displacement to mimic an oil-depleted state. These studies led to consistent conclusions that the hydrophobic system exhibits a significantly different drying pattern than the hydrophilic system, including drying rate, salt morphology, and salt distribution. In the hydrophobic pore system, there is no connected liquid film due to the hydrophobic grain surfaces, which inhibits the flow of residual brine to form intensive local salt precipitation and leads to less and homogeneous salt precipitation. Moreover, the salts tend to grow into large crystals due to slow drying rate and sufficient salt diffusion within the isolated brine pools (Fig.9; He et al., 2019; 2022). In contrast, the hydrophilic system generally presents intense local salt precipitation of polycrystalline salt aggregates. In the neutral system, the precipitated salts have characteristics that are intermediate between those of the hydrophobic and hydrophilic systems.

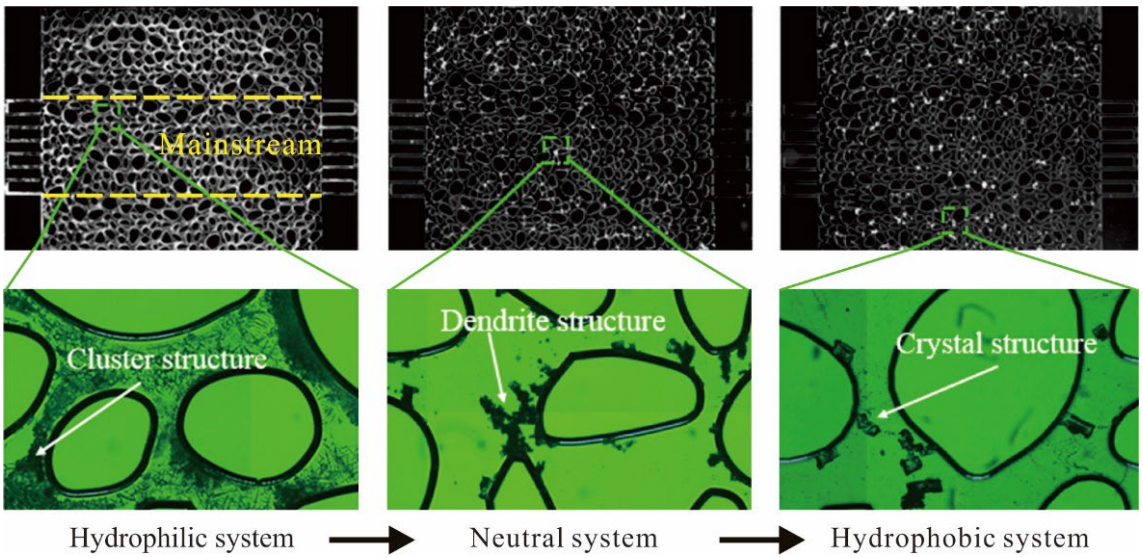

Fig. 9. Effect of rock wettability on salt precipitation: the hydrophilic system features intensive local salt precipitation of polycrystalline salt aggregates, the hydrophobic system is characterized by isolated large salt crystals, and the precipitated salts in the neutral system have characteristics that are intermediate between the other two systems, modified from He et al. (2019).

4.3 Gas aspect

4.3.1 CO_2 phase state

In contrast to the extensive research on the effects of brine and rock characteristics on salt precipitation during CO_2 storage, experimental studies focusing on gas properties are much scarcer. CO_2 exists in a supercritical state at temperatures greater than 31.1°C and pressures greater than 7.38 MPa, exhibiting gas-like viscosity and liquid-like density. To ensure commercial feasibility, a suitable storage site must meet the temperature and pressure conditions to maintain CO_2 in a supercritical state (Bachu, 2000, 2003). Thus, most experiments dedicated to salt precipitation during CO_2 storage have been carried out under conditions beyond the critical point of CO_2. However, some experiments have used gaseous CO_2 due to the limitations of experimental apparatuses (e.g., Kim et al., 2013; Van Hemert et al., 2013; Roels et al., 2014, 2016; Miri et al., 2015; Seo et al., 2019; Falcon-Suarez et al., 2020; Hu et al., 2022). To the best of our knowledge, studies addressing the effect of CO_2 phase states on salt precipitation are extremely scarce. Nooraiepour et al. (2018) conducted a microfluidic-chip experiment using a fractured caprock sample and considering gaseous, liquid and supercritical states of CO_2. Their study shows that CO_2 phase states influence the magnitude, distribution and precipitation pattern of local salt precipitation (Fig. 10). Compared to liquid and supercritical CO_2, gaseous CO_2 flushes less brine out of the fracture network, resulting in higher residual brine saturation due to lower imposed viscous forces. Thus, a higher amount of available brine leads to a greater accumulation of salt precipitation in the fracture. Moreover, CO_2 phase states affect the relationship between injection rate and salt accumulation, and flow rate exerts a more significant effect on $scCO_2$ than gaseous CO_2 (Nooraiepour et al., 2018). They suggested that further research is needed to determine the interdependence among CO_2 phase state, critical injection rate, and thermodynamic conditions of salt precipitation during CO_2 storage.

4.3.2 Gas composition

Some core or microfluidic-chip flooding experiments have used N_2/He/air instead of CO_2 in salt precipitation studies. This was done to avoid equipment corrosion by dissolved CO_2 and thus reduce the

leakage risk during flooding experiments (Peysson et al., 2011b, 2014; Peysson, 2012; Rufai and Crawshaw, 2018; Lopez et al., 2020; Mascle et al., 2023). It is unknown whether the different gas types have significant effects on salt precipitation due to the lack of controlled experiments using different gases. Rufai and Crawshaw (2018) conducted a microfluidic-chip experiment to compare the drying in a gaseous CO_2-brine system and an air-brine system. They found that the CO_2 case makes the system more water-wetting, which allows for a longer hydraulic connectivity to maintain a high evaporation rate stage in the CO_2-brine system (Fig. 11A). However, Heath et al. (2014) performed a pore-scale numerical simulation study to compare the fluid states between the CO_2-water system under CO_2 sequestration conditions and the air-water system in the vadose zone. They found that water adsorption and capillary condensation are weaker in the CO_2-water system than in the air-water system due to the lower surface tension and thinner liquid water films of the former system. Further experimental studies are required to better understand the effect of gas types on fluid water states and salt precipitation.

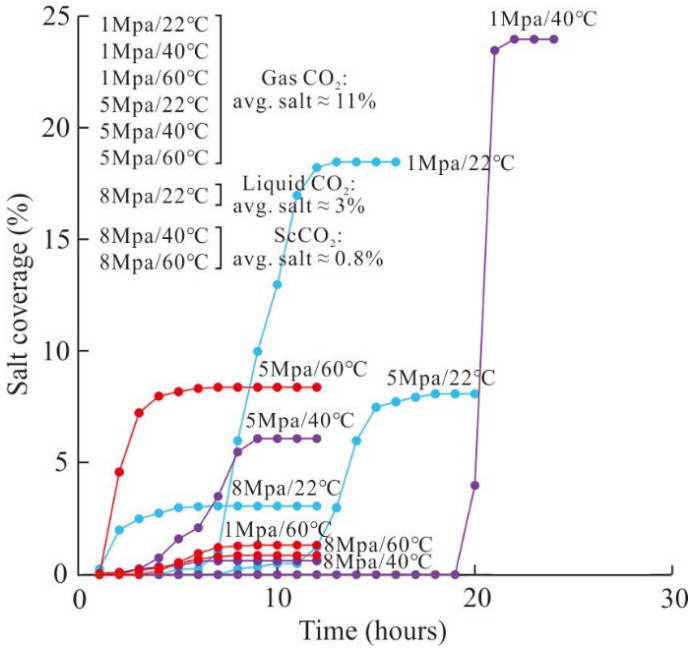

Fig. 10. Effect of gas phase states on salt precipitation, indicating that using gaseous CO_2 results in higher residual brine saturation and thus a greater accumulation of salt precipitation than using liquid and supercritical CO_2, modified from Nooraiepour et al. (2018).

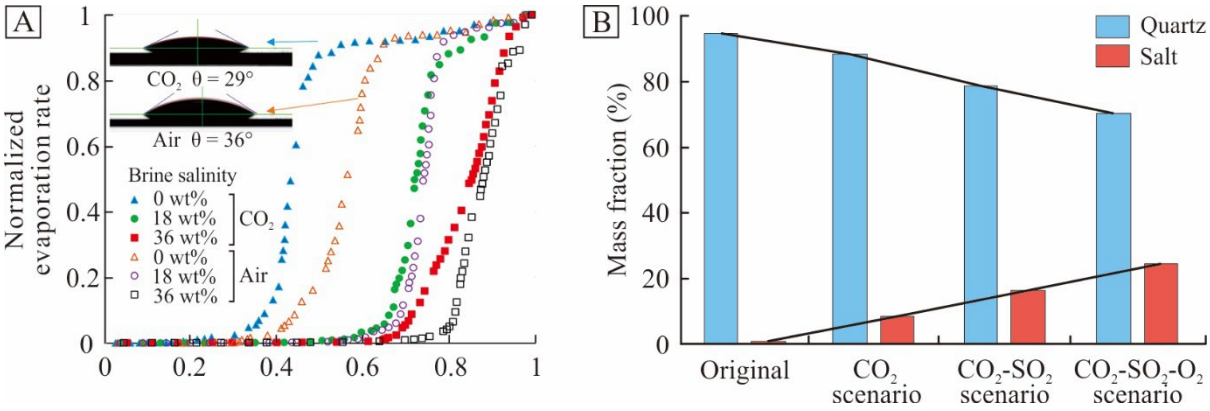

Fig. 11. Effect of gas composition on salt precipitation: (A) the high evaporation rate stage in the CO_2-brine system is longer than that of the air-brine system, modified from Rufai and Crawshaw (2018), and the existence of SO_2 and O_2 impurities in injected CO_2 results in more salt precipitation, modified from Wang et al. (2016).

Different impurities may be present in the captured CO_2, such as H_2S, SO_2, N_2, O_2, etc., depending on the different capture technologies and CO_2 sources (Porter et al., 2015). Removing these impurities from the CO_2 stream would increase energy consumption and operating costs. In addition, some impurity species are chemically reactive with capture, transport and injection facilities as well as with storage reservoirs (Razak et al., 2023). Thus, the potential reactions caused by reactive impurities need to be investigated. Several static batch experiments designed for CO_2-impurity-brine-rock interactions have documented salt precipitation. Bolourinejad and Herber (2013) employed different gas compositions to react with the same brine and rock. They found that the pure CO_2 scenario has a significant increase in permeability due to mineral dissolution, while the CO_2+100 ppm H_2S scenario has an almost unvaried permeability as halite and other mineral precipitation offsets mineral dissolution. In contrast, the CO_2+5000 ppm H_2S scenario shows a dramatic decrease in permeability. This is because the precipitation of pyrite and anhydrite provides more nucleation sites for halite precipitation. Wang et al. (2016) found the coexistence of stronger quartz dissolution and salt precipitation in the presence of SO_2 and O_2 impurities (Fig. 11B). They provided an alternative explanation that the SO_2 impurity enhances quartz dissolution and thus the formation of H_4SiO_4 when the brine is undersaturated with silica. This consumes water molecules that can interact with salt ions in highly concentrated brine, and hence increases salt concentrations. A numerical simulation study reported that the presence of SO_2 impurity accelerates silica dissolution, carbonate precipitation and additional sulfate precipitation. These together lead to a reduction in reservoir porosity and permeability (Waldmann et al., 2016). Overall, different studies have proposed different mechanisms for the effect of active gas impurities on salt precipitation and pore structure changes. However, they all agree that the presence of active impurities complicates gas-brine-rock interactions and thus exacerbates mineral precipitation and pore structure degradation.

4.4 Injection scenario aspect

4.4.1 Injection rate

The injection rate is one of the most critical factors controlling drying during CO_2 injection. A number of experimental studies focus exclusively or partially on this issue (e.g., Peysson et al., 2014; Ott et al., 2015; Jeddizahed and Rostami, 2016; Nooraiepour et al., 2018; He et al., 2019, 2022; Md Yusof et al., 2020; Akindipe et al., 2021; Mascle et al., 2023; Sokama-Neuyam et al., 2023). Increasing injection rate means higher viscous force, which drives more brine out of samples and inhibits capillary back-flow of brine. This results in higher displacement production of mobile brine and lower vapor production of residual brine (Fig. 12). Meanwhile, increasing injection rate also indicates a higher evaporation rate but a shorter evaporation period. As discussed in Section 3.2, salt precipitation presents a semi-homogeneous to a heterogeneous to a homogeneous distribution pattern with the increasing injection rate due to the balance of capillary back-flow, water evaporation, salt precipitation, and salt diffusion (Miri and Hellevang, 2016). Moreover, salt precipitation can form bulk large crystals at a low injection rate while micro-salt aggregates tend to form at a high injection rate due to fast evaporation and nucleation rates (He et al., 2022).

Many numerical studies have been performed to verify the effects of injection rate (e.g., Beni et al., 2011; Kim et al., 2012, 2014; André et al., 2014; Wang and Liu, 2014; Wang et al., 2017; Ghafoori et al., 2017; Cui et al., 2018a, 2018b; Piao et al., 2018; Parvin et al., 2020; Ren and Feng, 2021; Norouzi et al., 2021; Zhao and Cheng, 2022). Most numerical studies agree with the experimental studies and have confirmed that a high injection rate reduces local salt precipitation. The effect of the injection rate is dynamic, and its impact is more obvious at the early stage of drying (Ren and Feng, 2021). Furthermore,

the increasing injection rate does not significantly change salt precipitation beyond a critical injection rate (Norouzi et al., 2021).

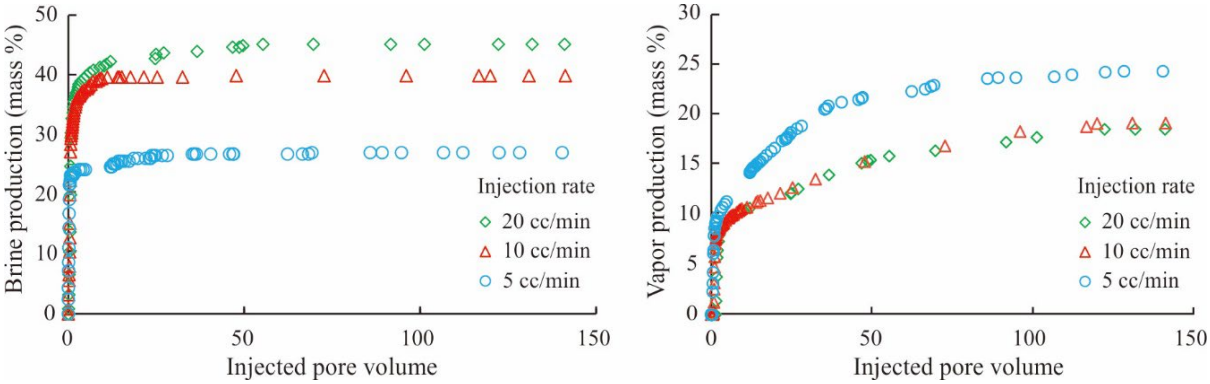

Fig. 12. Effect of injection rate on brine displacement and evaporation, indicating that increasing injection rates result in higher displacement production, less residual brine, and thus lower vapor production, modified from Jeddizahed and Rostami (2016).

4.4.2 Injection strategy

In order to reduce salt precipitation, and thus injectivity impairment, pre-, co- or post-injection of fresh or low-salinity water is the common treatment apart from selecting high-quality reservoirs and high injection rates (Fang et al., 2014; Wang and Liu, 2014; Cui et al., 2016, 2017; Miri and Hellevang, 2016; Zhang et al., 2016; Seo et al., 2019; Munkejord et al., 2021). Using a microfluidic experiment, Seo et al. (2019) found that sequential water injection with CO_2 for in-situ generation of micro-sized CO_2 bubbles can minimize drying and accelerate CO_2 dissolution. In addition, numerical studies also verified that using fresh or low-salinity water can reduce the amount of salt solute available for salt precipitation near injection wells (Cui et al., 2016; Zhang et al., 2016; Munkejord et al., 2021). However, for the pre-injection of water, it is still unknown whether the remaining brine in low-permeability interlayers and the brine replenishment from further areas can lead to salt precipitation during the subsequent injection of CO_2. For the co- or post-injection of water scenarios, acidic water formed by CO_2 dissolution can cause mineral dissolution and porosity increment. However, mineral precipitation and/or fines release, especially in carbonate-cemented rocks, will cause severe reservoir degradation. Several experimental studies have confirmed that fines mobilization appears to pose a greater threat to reservoir permeability, and the impairment increases dramatically when salt precipitation and fines mobilization occur simultaneously (Sokama-Neuyam et al., 2017a, 2017b; Sokama-Neuyam and Ursin, 2018; Wang et al., 2019; Md Yusof et al., 2020). For instance, Wang et al. (2019) determined the pore structure variations before and after core flooding based on the T_2 distribution of nuclear magnetic resonance (NMR) test. They found that the pore-throat blockage is worse in the injection scenario of CO_2-brine alternate flooding due to the coexistence of salt precipitation and fines mobilization (Fig. 13). Thus, the mitigation method for different storage reservoirs should be derived from a case-by-case analysis based on the comprehensive analysis of all geological and engineering factors, which will be discussed in the next section.

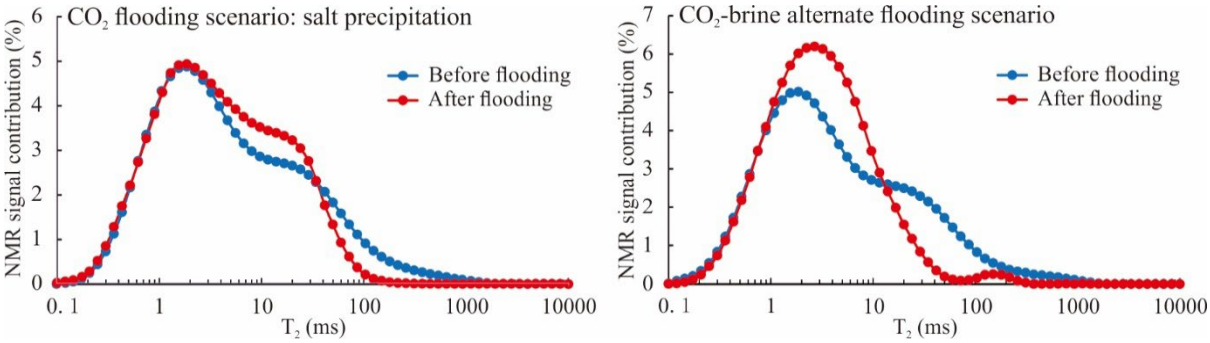

Fig. 13. Effects of injection scenarios on pore structure (T_2 reflects pore size, and NMR signal contribution reflects volume contribution of specific pore size), indicating that CO_2-brine alternate flooding scenario causes greater damage to pore structure due to the joint action of salt precipitation and fines mobilization, modified from Wang et al. (2019).

4.5 Combinatorial control of various factors

Although there are differences in how and to what extent different controlling factors affect salt precipitation and injectivity impairment, these factors tend to interact and determine the final outcome. Reservoir injectivity loss is mainly controlled by the amount and location of salt precipitation. Salt saturation is directly affected by brine salinity and brine source, which determine the salt content per unit volume and the brine volume available for evaporation and precipitation, respectively. Brine salinity is an intrinsic property of reservoirs, and can only be altered by injection of fresh or low-salinity water. Brine source includes both in-situ and ex-situ, and is the combined result of reservoir and engineering factors. The initial reservoir and permeability not only determine the residual brine saturation, i.e., in-situ brine for evaporation and precipitation, but also control the injection rate, i.e., high injection rate in high-permeability reservoir at the same injection pressure condition. Reservoir heterogeneity at the micro- and macro scales affects the ex-situ brine source for continuous salt precipitation. Rock wettability controls not only the in-situ residual brine saturation, but more importantly the transport pathways of ex-situ brine to the evaporation front. For low-salinity homogeneous reservoirs, a high injection rate of supercritical CO_2 may be sufficient to avoid extensive salt precipitation and injectivity loss. For high-salinity homogeneous reservoirs, a pre-flooding of fresh or low-salinity water prior to CO_2 injection could be an effective mitigation method. However, for highly heterogeneous hydrophilic reservoirs, other injection scenarios should be tested and verified, such as wettability modification and periodic injection of fresh or low-salinity water, combined with a high injection rate of supercritical CO_2.

5 Summary and conclusions

This paper presents a state-of-the-art review of the experimental studies on salt precipitation in the context of CO_2 storage. Using four experimental simulation systems for salt precipitation, namely core-flooding, microfluidic-chip, static batch, and surface drying experimental systems, the processes and distribution patterns of salt precipitation have been extensively investigated. Salt precipitation during CO_2 injection involves a complex interplay of various processes, including two-phase displacement of brine by CO_2, water evaporation, capillary backflow of brine, salt solute diffusion and salt nucleation and growth. Three distinct drying regimes, namely the diffusive regime, capillary regime, and evaporation regime, are determined by the coupling of brine loss during evaporation, brine replenishment due to capillary backflow, and salt diffusion homogenization. The drying regimes control three general macro-distribution patterns

of salt precipitation at the reservoir scale: the semi-homogeneous, heterogeneous, and homogeneous distribution patterns. Two main types of salt crystal morphologies have been identified in many experimental studies, namely large buck salt crystals and polycrystalline salt aggregates. However, there is still some debate regarding the micro-distribution of salt crystals at the pore scale. For example, it is controversial whether salt crystals are mainly distributed in small or large pore throats. And the salt self-enhancement mechanism proposed from microfluidic experiments needs to be proven using core-flooding experiments, to clarify if and how salt crystals can penetrate the CO_2-brine interfaces. These issues need to be further investigated as they determine the extent and way of reservoir pore structure degradation and hence CO_2 migration pathways.

More importantly, this paper presents a comprehensive analysis of the controlling factors for salt precipitation during CO_2 injection. Brine salinity, CO_2 injection rate and initial reservoir properties are considered the most critical in determining the amount and distribution of precipitated salts and the degree of injectivity impairment. It is commonly acknowledged that low salinity, high injection rate and high reservoir permeability can mitigate salt precipitation and its negative effect on reservoir injectivity. In addition, a relatively homogeneous pore and reservoir structure along with a hydrophobic feature of rock can reduce the likelihood of significant local salt precipitation. However, the coupling effects of heterogeneous reservoir structure, pore structure and wettability need to be investigated using specially designed experimental samples. Moreover, previous studies documented that there is relatively weak salt precipitation at the conditions of brine dominated by the monovalent salts and CO_2 in the supercritical phase without reactive impurities. However, experimental studies focusing on the effects of brine and gas compositions and CO_2 phase states are relatively scarce. Finally, it is particularly important to emphasize that although extensive laboratory work has been conducted to investigate the mechanism, distribution and controlling factors of salt precipitation during CO_2 injection, the most commonly used core-flooding and microfluidic experimental systems have a critical limitation in terms of sample size when compared to real reservoirs. In this case, the ex-situ brine replenishment may have been significantly underestimated, which could have resulted in an underestimation of the volume of local salts and a misunderstanding of the drying process. Therefore, the experimental systems must be improved to better mimic formation drying in the presence of different brine sources by using large samples or co-injecting gas and brine, as has been done in a few experimental studies.

Declaration of Competing Interest

The authors declare that they have no known competing financial interests or personal relationships that could have appeared to influence the work reported in this paper.

Data availability

Data will be made available on request.

Acknowledgments

Funding was provided by China University of Petroleum (East China) to the Independent Innovation Research Project 22CX06004A, by the Qingdao Municipal Bureau of Science and Technology to the Natural Science Project 23-2-1-55-zyyd-jch, by the Department of Science & Technology of Shandong

Province to the Natural Science Project ZR2023QD093, and by the National Natural Science Foundation of China to the Natural Science Project 42402140. SA acknowledges the Open Research Project SKLDOG2024-KFYB-02 funded by the State Key Laboratory of Deep Oil and Gas and the Research Team Cultivation Program 2023QNT004 funded by Shenzhen University. HH acknowledges funding from Norway Grants (UMO2019/34/H/ST10/00564) and EEA and Norway Grants (NOR/POLNORCCS/AGaStor/0008/2019-00). JA acknowledges funding from MICIU/AEI/10.13039/501100011033 and "ERDF/EU" (PID2022-140850OB-C22). AT acknowledges Grant PID2021-12246NB-C22 funded by MICIU/AEI/10.13039/501100011033, FEDER, EU, and the Catalan Council to the Grup Consolidat de Recerca Reconegut Geologia Sedimentària (2021 SGR-Cat 00349). EGR acknowledges funding from the DGICYT Spanish Project PID-2020-118999GB-I00 funded by MCIN/AEI/10.13039/501100011033) and the "Consolidación Investigadora" Grant CNS2023-145382 funded by MCIN/AEI/10.13039/50110001103 and European Union NextGeneration EU/PRTR.

References

Abbasi, P., Madani, M., Abbasi, S., Moghadasi, J., 2022. Mixed salt precipitation and water evaporation during smart water alternative CO2 injection in carbonate reservoirs. Journal of Petroleum Science and Engineering 208, 109258. https://doi.org/10.1016/j.petrol.2021.109258

Akindipe, D., Saraji, S., Piri, M., 2022. Salt precipitation in carbonates during supercritical CO2 injection: A pore-scale experimental investigation of the effects of wettability and heterogeneity. International Journal of Greenhouse Gas Control 121, 103790. https://doi.org/10.1016/j.ijggc.2022.103790

Akindipe, D., Saraji, S., Piri, M., 2021. Salt precipitation during geological sequestration of supercritical CO2 in saline aquifers: A pore-scale experimental investigation. Advances in Water Resources 155, 104011. https://doi.org/10.1016/j.advwatres.2021.104011

Alcalde, J., Flude, S., Wilkinson, M., Johnson, G., Edlmann, K., Bond, C.E., Scott, V., Gilfillan, S.M.V., Ogaya, X., Haszeldine, R.S., 2018. Estimating geological CO_2 storage security to deliver on climate mitigation. Nature Communications 9, 2201. https://doi.org/10.1038/s41467-018-04423-1

Alcalde, J., Heinemann, N., James, A., Bond, C.E., Ghanbari, S., Mackay, E.J., Haszeldine, R.S., Faulkner, D.R., Worden, R.H., Allen, M.J., 2021. A criteria-driven approach to the CO_2 storage site selection of East Mey for the acorn project in the North Sea. Marine and Petroleum Geology 133, 105309. https://doi.org/10.1016/j.marpetgeo.2021.105309

Aminu, M.D., Nabavi, S.A., Rochelle, C.A., Manovic, V., 2017. A review of developments in carbon dioxide storage. Applied Energy 208, 1389–1419. https://doi.org/10.1016/j.apenergy.2017.09.015

André, L., Peysson, Y., Azaroual, M., 2014. Well injectivity during CO2 storage operations in deep saline aquifers – Part 2: Numerical simulations of drying, salt deposit mechanisms and role of capillary forces. International Journal of Greenhouse Gas Control 22, 301–312. https://doi.org/10.1016/j.ijggc.2013.10.030

Bacci, G., Durucan, S., Korre, A., 2013. Experimental and numerical study of the effects of halite scaling on injectivity and seal performance during CO2 injection in saline aquifers. Energy Procedia 37, 3275–3282. https://doi.org/10.1016/j.egypro.2013.06.215

Bacci, G., Korre, A., Durucan, S., 2011. Experimental investigation into salt precipitation during CO2 injection in saline aquifers. Energy Procedia 4, 4450–4456. https://doi.org/10.1016/j.egypro.2011.02.399

Bachu, S., 2003. Screening and ranking of sedimentary basins for sequestration of CO2 in geological media in

response to climate change. Environmental Geology 44, 277–289. https://doi.org/10.1007/s00254-003-0762-9

Bachu, S., 2000. Sequestration of CO2 in geological media: Criteria and approach for site selection in response to climate change. Energy Conversion and Management 41, 953–970. https://doi.org/10.1016/S0196-8904(99)00149-1

Baumann, G., Henninges, J., De Lucia, M., 2014. Monitoring of saturation changes and salt precipitation during CO2 injection using pulsed neutron-gamma logging at the Ketzin pilot site. International Journal of Greenhouse Gas Control 28, 134–146. https://doi.org/10.1016/j.ijggc.2014.06.023

Beni, A.N., Clauser, C., Erlstrom, M., 2011. System analysis of underground CO2 storage by numerical modeling for a case study in Malmo. American Journal of Science 311, 335–368. https://doi.org/10.2475/04.2011.03

Bernachot, I., Garcia, B., Ader, M., Peysson, Y., Rosenberg, E., Bardoux, G., Agrinier, P., 2017. Solute transport in porous media during drying: The chlorine isotopes point of view. Chemical Geology 466, 102–115. https://doi.org/10.1016/j.chemgeo.2017.05.024

Berntsen, A., Todorovic, J., Raphaug, M., Torsæter, M., Chavez Panduro, E.A., Gawel, K., 2019. Salt clogging during supercritical CO2 injection into a downscaled borehole model. International Journal of Greenhouse Gas Control 86, 201–210. https://doi.org/10.1016/j.ijggc.2019.04.009

Black, J.R., Carroll, S.A., Haese, R.R., 2015. Rates of mineral dissolution under CO2 storage conditions. Chemical Geology 399, 134–144. https://doi.org/10.1016/j.chemgeo.2014.09.020

Bolourinejad, P., Herber, M.A., 2013. Experimental and modeling study of salt precipitation during injection of CO2 contaminated with H2S into depleted gas fields in Northeast Netherlands. All Days. SPE, 688–701. https://doi.org/10.2118/164932-MS

Budinis, S., Krevor, S., Dowell, N. Mac, Brandon, N., Hawkes, A., 2018. An assessment of CCS costs, barriers and potential. Energy Strategy Reviews 22, 61–81. https://doi.org/10.1016/j.esr.2018.08.003

Bui, M., Adjiman, C.S., Bardow, A., Anthony, E.J., Boston, A., Brown, S., Fennell, P.S., Fuss, S., Galindo, A., Hackett, L.A., Hallett, J.P., Herzog, H.J., Jackson, G., Kemper, J., Krevor, S., Maitland, G.C., Matuszewski, M., Metcalfe, I.S., Petit, C., Puxty, G., Reimer, J., Reiner, D.M., Rubin, E.S., Scott, S.A., Shah, N., Smit, B., Trusler, J.P.M., Webley, P., Wilcox, J., Mac Dowell, N., 2018. Carbon capture and storage (CCS): the way forward. Energy & Environmental Science 11, 1062–1176. https://doi.org/10.1039/C7EE02342A

Chasset, C., Jarsjö, J., Erlström, M., Cvetkovic, V., Destouni, G., 2011. Scenario simulations of CO2 injection feasibility, plume migration and storage in a saline aquifer, Scania, Sweden. International Journal of Greenhouse Gas Control 5, 1303–1318. https://doi.org/10.1016/j.ijggc.2011.06.003

Cui, G., Ren, S., Dou, B., Ning, F., 2021. Geothermal energy exploitation from depleted high-temperature gas reservoirs by recycling CO2: The superiority and existing problems. Geoscience Frontiers 12, 101078. https://doi.org/10.1016/j.gsf.2020.08.014

Cui, G., Ren, S., Rui, Z., Ezekiel, J., Zhang, L., Wang, H., 2018a. The influence of complicated fluid-rock interactions on the geothermal exploitation in the CO2 plume geothermal system. Applied Energy 227, 49–63. https://doi.org/10.1016/j.apenergy.2017.10.114

Cui, G., Wang, Y., Rui, Z., Chen, B., Ren, S., Zhang, L., 2018b. Assessing the combined influence of fluid-rock interactions on reservoir properties and injectivity during CO2 storage in saline aquifers. Energy 155, 281–296. https://doi.org/10.1016/j.energy.2018.05.024

Cui, G., Zhang, L., Ren, B., Enechukwu, C., Liu, Y., Ren, S., 2016. Geothermal exploitation from depleted high temperature gas reservoirs via recycling supercritical CO2: Heat mining rate and salt precipitation

effects. Applied Energy 183, 837–852. https://doi.org/10.1016/j.apenergy.2016.09.029

Cui, G., Zhang, L., Ren, S., 2017. Combined effects of geochemical reactions and salt precipitation on geothermal exploitation in the CPG system. Energy Procedia 105, 1276–1281. https://doi.org/10.1016/j.egypro.2017.03.455

Dai, Y., Lai, F., Ni, J., Liang, Y., Shi, H., Shi, G., 2022. Evaluation of the impact of CO2 geological storage on tight oil reservoir properties. Journal of Petroleum Science and Engineering 212, 110307. https://doi.org/10.1016/j.petrol.2022.110307

Dashtian, H., Shokri, N., Sahimi, M., 2018. Pore-network model of evaporation-induced salt precipitation in porous media: The effect of correlations and heterogeneity. Advances in Water Resources 112, 59–71. https://doi.org/10.1016/j.advwatres.2017.12.004

Edem, D.E., Abba, M.K., Nourian, A., Babaie, M., Naeem, Z., 2022. Experimental study on the interplay between different brine types/concentrations and CO2 injectivity for effective CO2 storage in deep saline aquifers. Sustainability (Switzerland) 14, 986. https://doi.org/10.3390/su14020986

Falcon-Suarez, I.H., Livo, K., Callow, B., Marin-Moreno, H., Prasad, M., Best, A.I., 2020. Geophysical early warning of salt precipitation during geological carbon sequestration. Scientific Reports 10, 16472. https://doi.org/10.1038/s41598-020-73091-3

Fang, Q., Li, Y., Cheng, P., Yu, Y., Liu, D., Song, S., 2014. Enhancing CO2 injectivity in high-salinity and low-permeability aquifers: A case study of Jianghan Basin, China. Earth Science-Journal of China University of Geosciences 39, 1575–1583. https://doi.org/10.3799/dqkx.2014.150

Ghafoori, M., Tabatabaei-Nejad, S.A., Khodapanah, E., 2017. Modeling rock-fluid interactions due to CO2 injection into sandstone and carbonate aquifer considering salt precipitation and chemical reactions. Journal of Natural Gas Science and Engineering 37, 523–538. https://doi.org/10.1016/j.jngse.2016.11.063

Golghanddashti, H., Saadat, M., Abbasi, S., Shahrabadi, A., 2013. Experimental investigation of water vaporization and its induced formation damage associated with underground gas storage. Journal of Porous Media 16, 89–96. https://doi.org/10.1615/JPorMedia.v16.i2.10

Grude, S., Landrø, M., Dvorkin, J., 2014. Pressure effects caused by CO2 injection in the Tubåen Fm., the Snøhvit field. International Journal of Greenhouse Gas Control 27, 178–187. https://doi.org/10.1016/j.ijggc.2014.05.013

Guyant, E., Han, W.S., Kim, K.Y., Park, M.H., Kim, B.Y., 2015. Salt precipitation and CO2/brine flow distribution under different injection well completions. International Journal of Greenhouse Gas Control 37, 299–310. https://doi.org/10.1016/j.ijggc.2015.03.020

Hajiabadi, S.H., Bedrikovetsky, P., Borazjani, S., Mahani, H., 2021. Well injectivity during CO2 geosequestration: A review of hydro-physical, chemical, and geomechanical effects. Energy and Fuels 35, 9240–9267. https://doi.org/10.1021/acs.energyfuels.1c00931

He, D., Jiang, P., Xu, R., 2023. The influence of heterogeneous structure on salt precipitation during CO2 geological storage. Advances in Geo-Energy Research 7, 189–198. https://doi.org/10.46690/ager.2023.03.05

He, D., Jiang, P., Xu, R., 2019. Pore-scale experimental investigation of the effect of supercritical CO2 injection rate and surface wettability on salt precipitation. Environmental Science & Technology 53, 14744–14751. https://doi.org/10.1021/acs.est.9b03323

He, D., Wang, Z., Yuan, H., Zhang, M., Hong, Z., Xu, R., Jiang, P., Chen, S., 2024. Experimental investigation of salt precipitation behavior and its impact on injectivity under variable injection operating conditions. Gas Science and Engineering 121, 205198.

https://doi.org/10.1016/j.jgsce.2023.205198

He, D., Xu, R., Ji, T., Jiang, P., 2022. Experimental investigation of the mechanism of salt precipitation in the fracture during CO2 geological sequestration. International Journal of Greenhouse Gas Control 118, 103693. https://doi.org/10.1016/j.ijggc.2022.103693

Heath, J.E., Bryan, C.R., Matteo, E.N., Dewers, T.A., Wang, Y., Sallaberry, C.J., 2014. Adsorption and capillary condensation in porous media as a function of the chemical potential of water in carbon dioxide. Water Resources Research 50, 2718–2731. https://doi.org/10.1002/2013WR013728

Ho, T.H.M., Tsai, P.A., 2020. Microfluidic salt precipitation: Implications for geological CO2 storage. Lab on a Chip 20, 3806–3814. https://doi.org/10.1039/d0lc00238k

Holzheid, A., 2016. Dissolution kinetics of selected natural minerals relevant to potential CO2-injection sites − Part 1: A review. Chemie Der Erde 76, 621–641. https://doi.org/10.1016/j.chemer.2016.09.007

Hu, X., Wang, J., Zhang, L., Xiong, H., Wang, Z., Duan, H., Yao, J., Sun, H., Zhang, L., Song, W., Zhong, J., 2022. Direct visualization of nanoscale salt precipitation and dissolution dynamics during CO2 injection. Energies 15, 9567. https://doi.org/10.3390/en15249567

IPCC, 2018. Global Warming of 1.5°C: An IPCC special report [WWW Document], Intergovernmental Panel on Climate Change. URL https://www.ipcc.ch/sr15/ (accessed 7.11.22).

Jayasekara, D.W., Ranjith, P.G., Wanniarachchi, W.A.M., Rathnaweera, T.D., Chaudhuri, A., 2020. Effect of salinity on supercritical CO2 permeability of caprock in deep saline aquifers: An experimental study. Energy 191, 116486. https://doi.org/10.1016/j.energy.2019.116486

Jeddizahed, J., Rostami, B., 2016. Experimental investigation of injectivity alteration due to salt precipitation during CO2 sequestration in saline aquifers. Advances in Water Resources 96, 23–33. https://doi.org/10.1016/j.advwatres.2016.06.014

Kaszuba, J., Yardley, B., Andreani, M., 2013. Experimental perspectives of mineral dissolution and precipitation due to carbon dioxide-water-rock interactions. Reviews in Mineralogy and Geochemistry 77, 153–188. https://doi.org/10.2138/rmg.2013.77.5

Kim, K.Y., Han, W.S., Kim, T., 2011. Numerical study of pressure evolution from CO2 injection in saline Aquifers. Energy Procedia 4, 4532–4537. https://doi.org/10.1016/j.egypro.2011.02.410

Kim, K.Y., Han, W.S., Oh, J., Kim, T., Kim, J.C., 2012. Characteristics of salt-precipitation and the associated pressure build-up during CO2 storage in saline aquifers. Transport in Porous Media 92, 397–418. https://doi.org/10.1007/s11242-011-9909-4

Kim, K.Y., Han, W.S., Oh, J., Park, E., Lee, P.K., 2014. Flow dynamics of CO2/brine at the interface between the storage formation and sealing units in a multi-layered model. Transport in Porous Media 105, 611–633. https://doi.org/10.1007/s11242-014-0387-3

Kim, M., Sell, A., Sinton, D., 2013. Aquifer-on-a-Chip: Understanding pore-scale salt precipitation dynamics during CO2 sequestration. Lab on a Chip 13, 2508–2518. https://doi.org/10.1039/c3lc00031a

Kumar, R., Campbell, S., Sonnenthal, E., Cunningham, J., 2020. Effect of brine salinity on the geological sequestration of CO2 in a deep saline carbonate formation. Greenhouse Gases: Science and Technology 10, 296–312. https://doi.org/10.1002/ghg.1960

Leung, D.Y.C., Caramanna, G., Maroto-Valer, M.M., 2014. An overview of current status of carbon dioxide capture and storage technologies. Renewable and Sustainable Energy Reviews 39, 426–443. https://doi.org/10.1016/j.rser.2014.07.093

Lima, M.G., Javanmard, H., Vogler, D., Saar, M.O., Kong, X.Z., 2021. Flow-through drying during CO2 injection into brine-filled natural fractures: A tale of effective normal stress. International Journal of Greenhouse Gas Control 109, 103378. https://doi.org/10.1016/j.ijggc.2021.103378

Lopez, O., Youssef, S., Estublier, A., Alvestad, J., Weierholt Strandli, C., 2020. Permeability alteration by salt precipitation: Numerical and experimental investigation using X-Ray Radiography. E3S Web of Conferences 146, 1–12. https://doi.org/10.1051/e3sconf/202014603001

Mascle, M., Lopez, O., Deschamps, H., Rennan, L., Lenoir, N., Tengattini, A., Youssef, S., 2023. Investigation of salt precipitation dynamic in porous media by X-ray and Neutron dual-modality imaging. In: Peysson, Y., Pironon, J. (Eds.), Science and Technology for Energy Transition 78, 11. https://doi.org/10.2516/stet/2023009

Masoudi, M., Fazeli, H., Miri, R., Hellevang, H., 2021. Pore scale modeling and evaluation of clogging behavior of salt crystal aggregates in CO2-rich phase during carbon storage. International Journal of Greenhouse Gas Control 111, 103475. https://doi.org/10.1016/j.ijggc.2021.103475

Mat Razali, N.Z., Mustapha, K.A., Kashim, M.Z., Misnan, M.S., Md Shah, S.S., Abu Bakar, Z.A., 2022. Critical rate analysis for CO2 injection in depleted gas field, Sarawak Basin, offshore East Malaysia. Carbon Management 13, 294–309. https://doi.org/10.1080/17583004.2022.2074312

Md Yusof, M.A., Ibrahim, M.A., Idress, M., Idris, A.K., M Saaid, I., Mohd Rodzi, N., Mohsin, S., Azhari Awangku Matali, A.A., 2020. Effects of CO2/rock/formation brine parameters on CO2 injectivity for sequestration. SPE Journal 26, 1455–1468. https://doi.org/10.4043/30157-MS

Md Yusof, M.A., Mohamed, M.A., Md Akhir, N.A., Ibrahim, M.A., Saaid, I.M., Idris, A.K., Idress, M., Awangku Matali, A.A.A., 2022. Influence of brine-rock parameters on rock physical changes during CO2 sequestration in saline aquifer. Arabian Journal for Science and Engineering 47, 11345–11359. https://doi.org/10.1007/s13369-021-06110-8

Messabeb, H., Contamine, F., Cézac, P., Serin, J.P., Pouget, C., Gaucher, E.C., 2017. Experimental measurement of CO2 solubility in aqueous CaCl2 solution at temperature from 323.15 to 423.15 K and pressure up to 20 MPa using the conductometric titration. Journal of Chemical and Engineering Data 62, 4228–4234. https://doi.org/10.1021/acs.jced.7b00591

Miri, R., Hellevang, H., 2016. Salt precipitation during CO2 storage-A review. International Journal of Greenhouse Gas Control 51, 136–147. https://doi.org/10.1016/j.ijggc.2016.05.015

Miri, R., van Noort, R., Aagaard, P., Hellevang, H., 2015. New insights on the physics of salt precipitation during injection of CO2 into saline aquifers. International Journal of Greenhouse Gas Control 43, 10–21. https://doi.org/10.1016/j.ijggc.2015.10.004

Muller, N., Qi, R., Mackie, E., Pruess, K., Blunt, M.J., 2009. CO2 injection impairment due to halite precipitation. Energy Procedia 1, 3507–3514. https://doi.org/10.1016/j.egypro.2009.02.143

Munkejord, S.T., Hammer, M., Ervik, Å., Odsæter, L.H., Lund, H., 2021. Coupled CO2-well-reservoir simulation using a partitioned approach: effect of reservoir properties on well dynamics. Greenhouse Gases: Science and Technology 11, 103–127. https://doi.org/10.1002/ghg.2035

Nachshon, U., Weisbrod, N., Dragila, M.I., Grader, A., 2011. Combined evaporation and salt precipitation in homogeneous and heterogeneous porous media. Water Resources Research 47, 1–16. https://doi.org/10.1029/2010WR009677

Ngata, M.R., Yang, B., Khalid, W., Ochilov, E., Mwakipunda, G.C., Aminu, M.D., 2023. Review on experimental investigation into formation damage during geologic carbon sequestration: Advances and outlook. Energy and Fuels 37, 6382–6400. https://doi.org/10.1021/acs.energyfuels.3c00427

Nooraiepour, M., Fazeli, H., Miri, R., Hellevang, H., 2018. Effect of CO2 phase states and flow rate on salt precipitation in shale caprocks - A microfluidic study. Environmental Science and Technology 52, 6050–6060. https://doi.org/10.1021/acs.est.8b00251

Norouzi, A.M., Babaei, M., Han, W.S., Kim, K.Y., Niasar, V., 2021. CO2-plume geothermal processes: A

parametric study of salt precipitation influenced by capillary-driven backflow. Chemical Engineering Journal 425, 130031. https://doi.org/10.1016/j.cej.2021.130031

Norouzi Rad, M., Shokri, N., 2014. Effects of grain angularity on NaCl precipitation in porous media during evaporation. Water Resources Research 50, 9020–9030. https://doi.org/10.1002/2014WR016125

Norouzi Rad, M., Shokri, N., Keshmiri, A., Withers, P.J., 2015. Effects of grain and pore size on salt precipitation during evaporation from porous media. Transport in Porous Media 110, 281–294. https://doi.org/10.1007/s11242-015-0515-8

Ott, H., Andrew, M., Snippe, J., Blunt, M.J., 2014. Microscale solute transport and precipitation in complex rock during drying. Geophysical Research Letters 41, 8369–8376. https://doi.org/10.1002/2014GL062266

Ott, H., De Kloe, K.D., Marcelis, F., Makurat, A., 2011. Injection of supercritical CO2 in brine saturated sandstone: Pattern formation during salt precipitation. Energy Procedia 4, 4425–4432. https://doi.org/10.1016/j.egypro.2011.02.396

Ott, H., Roels, S.M., de Kloe, K., 2015. Salt precipitation due to supercritical gas injection: I. Capillary-driven flow in unimodal sandstone. International Journal of Greenhouse Gas Control 43, 247–255. https://doi.org/10.1016/j.ijggc.2015.01.005

Ott, H., Snippe, J., de Kloe, K., 2021. Salt precipitation due to supercritical gas injection: II. Capillary transport in multi porosity rocks. International Journal of Greenhouse Gas Control 105, 103233. https://doi.org/10.1016/j.ijggc.2020.103233

Ott, H., Snippe, J., De Kloe, K., Husain, H., Abri, A., 2013. Salt precipitation due to sc-gas injection: Single versus multi-porosity rocks. Energy Procedia 37, 3319–3330. https://doi.org/10.1016/j.egypro.2013.06.220

Parvin, S., Masoudi, M., Sundal, A., Miri, R., 2020. Continuum scale modelling of salt precipitation in the context of CO2 storage in saline aquifers with MRST compositional. International Journal of Greenhouse Gas Control 99, 103075. https://doi.org/10.1016/j.ijggc.2020.103075

Peysson, Y., 2012. Permeability alteration induced by drying of brines in porous media. The European Physical Journal Applied Physics 60, 24206. https://doi.org/10.1051/epjap/2012120088

Peysson, Y., André, L., Azaroual, M., 2014. Well injectivity during CO2 storage operations in deep saline aquifers-Part 1: Experimental investigation of drying effects, salt precipitation and capillary forces. International Journal of Greenhouse Gas Control 22, 291–300. https://doi.org/10.1016/j.ijggc.2013.10.031

Peysson, Y., Bazin, B., Magnier, C., Kohler, E., Youssef, S., 2011a. Permeability alteration due to salt precipitation driven by drying in the context of CO2 injection. Energy Procedia 4, 4387–4394. https://doi.org/10.1016/j.egypro.2011.02.391

Peysson, Y., Fleury, M., Blázquez-Pascual, V., 2011b. Drying rate measurements in convection- and diffusion-driven conditions on a shaly sandstone using nuclear magnetic resonance. Transport in Porous Media 90, 1001–1016. https://doi.org/10.1007/s11242-011-9829-3

Piao, J., Han, W.S., Choung, S., Kim, K.-Y., 2018. Dynamic behavior of CO2 in a wellbore and storage formation: Wellbore-coupled and salt-precipitation processes during geologic CO2 sequestration. Geofluids 2018, 1–20. https://doi.org/10.1155/2018/1789278

Porter, R.T.J., Fairweather, M., Pourkashanian, M., Woolley, R.M., 2015. The range and level of impurities in CO2 streams from different carbon capture sources. International Journal of Greenhouse Gas Control 36, 161–174. https://doi.org/10.1016/j.ijggc.2015.02.016

Qi, R., Laforce, T.C., Blunt, M.J., 2009. A three-phase four-component streamline-based simulator to study

carbon dioxide storage. Computational Geosciences 13, 493–509. https://doi.org/10.1007/s10596-009-9139-9

Rathnaweera, T.D., Ranjith, P.G., Perera, M.S.A., 2016. Experimental investigation of geochemical and mineralogical effects of CO2 sequestration on flow characteristics of reservoir rock in deep saline aquifers. Scientific Reports 6, 1–12. https://doi.org/10.1038/srep19362

Rathnaweera, T.D., Ranjith, P.G., Perera, M.S.A., Ranathunga, A.S., Wanniarachchi, W.A.M., Yang, S.Q., Lashin, A., Al Arifi, N., 2017. An experimental investigation of coupled chemico-mineralogical and mechanical changes in varyingly-cemented sandstones upon CO2 injection in deep saline aquifer environments. Energy 133, 404–414. https://doi.org/10.1016/j.energy.2017.05.154

Razak, A.A., M Saaid, I., Md Yusof, M.A., Husein, N., Zaidin, M.F., Mohamad Sabil, K., 2023. Physical and chemical effect of impurities in carbon capture, utilisation and storage. Journal of Petroleum Exploration and Production Technology 13, 1235–1246. https://doi.org/10.1007/s13202-023-01616-3

Ren, J., Feng, D., 2021. Sensitivity analysis strategy to assess the salting-out problem during CO2 geological storage process. In: Cheng, Z. (Ed.), Shock and Vibration 2021, 1–14. https://doi.org/10.1155/2021/2809467

Ren, J., Wang, Y., Feng, D., Gong, J., 2022. Characterization method and spplication of heterogeneous reservoir based on different data quantity. In: Wu, Y. (Ed.), Lithosphere 2021, 8267559. https://doi.org/10.2113/2022/8267559

Ren, J., Wang, Y., Zhang, Y., 2018. A numerical simulation of a dry-out process for CO2 sequestration in heterogeneous deep saline aquifers. Greenhouse Gases: Science and Technology 8, 1090–1109. https://doi.org/10.1002/ghg.1821

Roels, S.M., El Chatib, N., Nicolaides, C., Zitha, P.L.J., 2016. Capillary-driven transport of dissolved salt to the drying zone during CO2 injection in homogeneous and layered porous media. Transport in Porous Media 111, 411–424. https://doi.org/10.1007/s11242-015-0601-y

Roels, S.M., Ott, H., Zitha, P.L.J., 2014. μ-CT analysis and numerical simulation of drying effects of CO2 injection into brine-saturated porous media. International Journal of Greenhouse Gas Control 27, 146–154. https://doi.org/10.1016/j.ijggc.2014.05.010

Rufai, A., Crawshaw, J., 2018. Effect of wettability changes on evaporation rate and the permeability impairment due to salt deposition. ACS Earth and Space Chemistry 2, 320–329. https://doi.org/10.1021/acsearthspacechem.7b00126

Rufai, A., Crawshaw, J., 2017. Micromodel observations of evaporative drying and salt deposition in porous media. Physics of Fluids 29. https://doi.org/10.1063/1.5004246

Seo, S., Mastiani, M., Hafez, M., Kunkel, G., Ghattas Asfour, C., Garcia-Ocampo, K.I., Linares, N., Saldana, C., Yang, K., Kim, M., 2019. Injection of in-situ generated CO2 microbubbles into deep saline aquifers for enhanced carbon sequestration. International Journal of Greenhouse Gas Control 83, 256–264. https://doi.org/10.1016/j.ijggc.2019.02.017

Sghaier, N., Prat, M., 2009. Effect of efflorescence formation on drying kinetics of porous media. Transport in Porous Media 80, 441–454. https://doi.org/10.1007/s11242-009-9373-6

Sokama-Neuyam, Y.A., Boakye, P., Aggrey, W.N., Obeng, N.O., Adu-Boahene, F., Woo, S.H., Ursin, J.R., 2020. Theoretical modeling of the impact of salt precipitation on CO2 storage potential in fractured saline reservoirs. ACS Omega 5, 14776–14785. https://doi.org/10.1021/acsomega.0c01687

Sokama-Neuyam, Y.A., Forsetløkken, S.L., Lien, J., Ursin, J.R., 2017a. The coupled effect of fines mobilization and salt precipitation on CO2 injectivity. Energies 10, 1125. https://doi.org/10.3390/en10081125

Sokama-Neuyam, Y.A., Ginting, P.U.R., Timilsina, B., Ursin, J.R., 2017b. The impact of fines mobilization on CO2 injectivity: An experimental study. International Journal of Greenhouse Gas Control 65, 195–202. https://doi.org/10.1016/j.ijggc.2017.08.019

Sokama-Neuyam, Y.A., Ursin, J.R., 2018. The coupled effect of salt precipitation and fines mobilization on CO2 injectivity in sandstone. Greenhouse Gases: Science and Technology 8, 1066–1078. https://doi.org/10.1002/ghg.1817

Sokama-Neuyam, Y.A., Ursin, J.R., Boakye, P., 2019. Experimental investigation of the mechanisms of salt precipitation during CO2 injection in sandstone. Journal of Carbon Research 5, 4. https://doi.org/10.3390/c5010004

Sokama-Neuyam, Y.A., Yusof, M.A.M., Owusu, S.K., Darkwah-Owusu, V., Turkson, J.N., Otchere, A.S., Ursin, J.R., 2023. Experimental and theoretical investigation of the mechanisms of drying during CO2 injection into saline reservoirs. Scientific Reports 13, 9155. https://doi.org/10.1038/s41598-023-36419-3

Sun, X., Alcalde, J., Bakhtbidar, M., Elío, J., Vilarrasa, V., Canal, J., Ballesteros, J., Heinemann, N., Haszeldine, S., Cavanagh, A., Vega-Maza, D., Rubiera, F., Martínez-Orio, R., Johnson, G., Carbonell, R., Marzan, I., Travé, A., Gomez-Rivas, E., 2021. Hubs and clusters approach to unlock the development of carbon capture and storage – Case study in Spain. Applied Energy 300, 117418. https://doi.org/10.1016/j.apenergy.2021.117418

Sun, X., Alcalde, J., Gomez-Rivas, E., Struth, L., Johnson, G., Travé, A., 2020. Appraisal of CO_2 storage potential in compressional hydrocarbon-bearing basins: Global assessment and case study in the Sichuan Basin (China). Geoscience Frontiers 11, 2309–2321. https://doi.org/10.1016/j.gsf.2020.02.008

Talman, S., Shokri, A.R., Chalaturnyk, R., Nickel, E., 2020. Salt precipitation at an active CO2 injection site. Gas Injection into Geological Formations and Related Topics. Wiley, 183–199. https://doi.org/10.1002/9781119593324.ch11

Tang, Y., Wang, N., He, Y., Wang, Y., Shan, Y., Zhang, H., Sun, Y., 2023. Impact of salt deposition induced by water evaporation on petrophysical properties and pore structure in underground gas storage through dynamic and static experiments. Journal of Hydrology 617, 129033. https://doi.org/10.1016/j.jhydrol.2022.129033

Tang, Y., Yang, R., Du, Z., Zeng, F., 2015. Experimental study of formation damage caused by complete water vaporization and salt precipitation in sandstone reservoirs. Transport in Porous Media 107, 205–218. https://doi.org/10.1007/s11242-014-0433-1

Torsæter, M., Cerasi, P., 2018. Geological and geomechanical factors impacting loss of near-well permeability during CO2 injection. International Journal of Greenhouse Gas Control 76, 193–199. https://doi.org/10.1016/j.ijggc.2018.07.006

Tsai, E.S., Jiang, H., Panagiotopoulos, A.Z., 2015. Monte Carlo simulations of H2O-CaCl2 and H2O-CaCl2-CO2 mixtures. Fluid Phase Equilibria 407, 262–268. https://doi.org/10.1016/j.fluid.2015.05.036

UNFCCC, 2022. Nationally Determined Contributions (NDCs) [WWW Document], United Nations Framework Convention on Climate Change. URL https://www4.unfccc.int/sites/NDCStaging/Pages/All.aspx (accessed 7.11.22).

Van Hemert, P., Rudolph, E.S.J., Zitha, P.L.J., 2013. Micro computer tomography study of potassium iodide precipitation in bentheimer sandstone caused by flow-through CO2 drying. Energy Procedia 37, 3331–3346. https://doi.org/10.1016/j.egypro.2013.06.221

Vanorio, T., Nur, A., Ebert, Y., 2011. Rock physics analysis and time-lapse rock imaging of geochemical effects due to the injection of CO2 into reservoir rocks. Geophysics 76, 23–33.

https://doi.org/10.1190/geo2010-0390.1

Waldmann, S., Hofstee, C., Koenen, M., Loeve, D., Liebscher, A., Neele, F., 2016. Physicochemical effects of discrete CO2-SO2 mixtures on injection and storage in a sandstone aquifer. International Journal of Greenhouse Gas Control 54, 640–651. https://doi.org/10.1016/j.ijggc.2016.07.026

Wang, Q., Yang, S., Han, H., Wang, L., Qian, K., Pang, J., 2019. Experimental investigation on the effects of CO2 displacement methods on petrophysical property changes of ultra-low permeability sandstone reservoirs near injection wells. Energies 12, 327. https://doi.org/10.3390/en12020327

Wang, Y., Liu, Y., 2014. Dry-out effect and site selection for CO2 storage in deep saline aquifers. Rock and Soil Mechanics 35, 1711–1717.

Wang, Y., Liu, Y., 2013. Impact of capillary pressure on permeability impairment during CO2 injection into deep saline aquifers. Journal of Central South University 20, 2293–2298. https://doi.org/10.1007/s11771-013-1736-z

Wang, Y., Luce, T., Ishizawa, C., Shuck, M., Smith, K., Ott, H., Appel, M., 2010. Halite precipitation and permeability assessment during supercritical CO2 core flood. International Symposium of the Society of Core Analysts. Halifax, Nova Scotia, Canada, 4–7.

Wang, Y., Mackie, E., Rohan, J., Luce, T., Knabe, R., Appel, M., 2009. Experimental study on halite precipitation during CO2 sequestration. International Symposium of the Society of Core Analysts. Noordwijk, The Netherlands, 1–12.

Wang, Y., Ren, J., Hu, S., Feng, D., 2017. Global sensitivity analysis to assess salt precipitation for CO2 geological storage in deep saline aquifers. Geofluids 2017, 1–16. https://doi.org/10.1155/2017/5603923

Wang, Z., Chen, S., Yuan, H., Hong, Z., Xu, R., Jiang, P., He, D., 2024. Experimental investigation on salt precipitation behavior during carbon geological sequestration: considering the influence of formation boundary solutions. Energy & Fuels 38, 514–525. https://doi.org/10.1021/acs.energyfuels.3c03767

Wang, Z., Wang, J., Lan, C., He, I., Ko, V., Ryan, D., Wigston, A., 2016. A study on the impact of SO2 on CO2 injectivity for CO2 storage in a Canadian saline aquifer. Applied Energy 184, 329–336. https://doi.org/10.1016/j.apenergy.2016.09.067

Zhang, D., Kang, Y., Selvadurai, A.P.S., You, L., 2020. Experimental investigation of the effect of salt precipitation on the physical and mechanical properties of a tight sandstone. Rock Mechanics and Rock Engineering 53, 4367–4380. https://doi.org/10.1007/s00603-019-02032-y

Zhang, L., Cui, G., Zhang, Y., Ren, B., Ren, S., Wang, X., 2016. Influence of pore water on the heat mining performance of supercritical CO2 injected for geothermal development. Journal of CO2 Utilization 16, 287–300. https://doi.org/10.1016/j.jcou.2016.08.008

Zhao, R., Cheng, J., 2022. Salt precipitation and associated pressure buildup during CO2 storage in heterogeneous anisotropy aquifers. Environmental Science and Pollution Research 29, 8650–8664. https://doi.org/10.1007/s11356-021-16322-y